

Journal Pre-proofs

Design, synthesis and anticonvulsant activity of new imidazolidindione and imidazole derivatives

Adel A. Marzouk, Amr K.A. Bass, Montaser Sh. Ahmed, Antar A. Abdelhamid, Yaseen A.M.M. Elshaier, Asmaa M.M. Salman, Omar M. Aly

PII: S0045-2068(20)31317-1
DOI: <https://doi.org/10.1016/j.bioorg.2020.104020>
Reference: YBIOO 104020

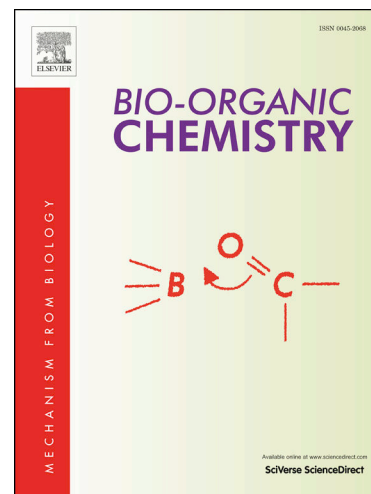
To appear in: *Bioorganic Chemistry*

Received Date: 22 November 2019
Revised Date: 6 June 2020
Accepted Date: 12 June 2020

Please cite this article as: A.A. Marzouk, A.K.A. Bass, M.S. Ahmed, A.A. Abdelhamid, Y.A.M. Elshaier, A.M.M. Salman, O.M. Aly, Design, synthesis and anticonvulsant activity of new imidazolidindione and imidazole derivatives, *Bioorganic Chemistry* (2020), doi: <https://doi.org/10.1016/j.bioorg.2020.104020>

This is a PDF file of an article that has undergone enhancements after acceptance, such as the addition of a cover page and metadata, and formatting for readability, but it is not yet the definitive version of record. This version will undergo additional copyediting, typesetting and review before it is published in its final form, but we are providing this version to give early visibility of the article. Please note that, during the production process, errors may be discovered which could affect the content, and all legal disclaimers that apply to the journal pertain.

© 2020 Elsevier Inc. All rights reserved.



Design, synthesis and anticonvulsant activity of new imidazolidindione and imidazole derivatives

Adel A. Marzouk^a, Amr K. A. Bass^b, Montaser Sh. Ahmed^a, Antar A. Abdelhamid^{c,d}, Yaseen A. M. M. Elshaier^e, Asmaa MM Salman^f, and Omar M. Aly^g

^a Department of Pharmaceutical Chemistry, Faculty of Pharmacy, Al-Azhar University, Assiut Branch, Egypt.

^b Department of Pharmaceutical Chemistry, Faculty of Pharmacy, Menoufia University, Egypt.

^c Department of Chemistry, Faculty of Science, Sohag University, Egypt.

^d Chemistry Department, Faculty of Science, Albaha University, Albaha (P.O. Box 1988), Saudi Arabia.

^e Department of Organic and Medicinal Chemistry, Faculty of Pharmacy, University of Sadat City, Sadat City, Menoufia, Egypt.

^f Medicinal and Pharmaceutical Chemistry Department, National Research Centre, Dokki, Cairo, Egypt.

^g Department of Medicinal Chemistry, Faculty of Pharmacy, Minia University, Egypt.

***Corresponding author:** e-mail; adelmarzouk@azhar.edu.eg, Tel.: +201021213733 address: Pharmaceutical Chemistry Department, Faculty of Pharmacy, Al-Azhar University, Assiut Branch, Egypt.

Abstract

New imidazolidindiones and tetra-substituted imidazole derivatives were designed, synthesized, and evaluated for the anticonvulsant activity through pentylenetetrazole (PTZ)-induced seizures and maximal electroshock (MES) tests using valproate sodium and phenytoin sodium as reference drugs, respectively. Most of the target compounds showed excellent activity against pentylenetetrazole (PTZ)-induced seizures with fair to no-activity against MES. Compounds **3d**, **4e**, **11b**, and **11e** showed higher activity (120 %) than that of valproate sodium in PTZ model. Almost all compounds showed no neurotoxicity, as indicated by the rotarod test. Estimation of physicochemical properties and pharmacokinetic profiles of the target compounds were studied. The chemical structures of the target compounds were characterized by different spectrometric methods and elemental analysis.

Keywords: Spiro[fluorene-9,4'-imidazolidine]; Imidazolidinediones, Imidazoles; Anticonvulsant Activity; Neurotoxicity; shape similarity.

1. Introduction

Epilepsy is a common neurological disease that affects about 50 million people of all ages in the world. Noteworthy, about 80% of them live in low- and middle-income countries. Epilepsy is diagnosed by recurrent seizure attacks which involve a group of symptoms that is spontaneous and intermittent with abnormal electrical activity in the brain accompanied by episodes of the motor, sensory or autonomic phenomenon. The attacks occur with or without loss of consciousness[1,2]. Currently, clinically available drugs produce acceptable seizure control in about 60 –70% of patients. Unfortunately, still, about 30% of patients suffer uncontrolled seizure attacks and they are pharmaco-resistant to the available therapy[3]. In addition, the available drugs have major side-effects, narrow therapeutic indices and difficulty to be formulated. The anticonvulsant drug must reach its receptors in the central nervous system to exert its therapeutic effect [4].

It is noticed that most of the antiepileptic drugs don't have any site of action or known mechanism of action[5]. The shortage of understanding and complexity of the mechanism of action certainly affects the development of new candidates as possible Anti-Epileptic Drugs (AEDs) through mechanism-driven designs. So, the design of a new antiepileptic drug depends on shape similarities as basic descriptors of computational drug discovery to model and the correct understanding of the protein-ligand interactions. Shape exhibits good neighboring behaviors, thus, similarities in the shape reflects similarities in biological activities most notably in 2D structures.

Also, calculations of molecular properties are very important in filtering new drug candidates as important tools to achieve good bioavailability[6]. Consideration of Lipinski rule known as Role of Five ((RO5)[7-10] and estimation of molecular polar surface area (PSA) or topological polar surface area (TPSA) are very important parameters for the prediction of drug transport properties[7]. Molecular polar surface area (PSA) is used to calculate the percentage of ABS using the expression: $\%ABS = 109 - 0.345 PSA$ [11].

Anti-epileptic research mainly focuses on the study of new anticonvulsant agents through conventional screening and structural modifications rather than mechanism-based drug design. So, drug identification is usually conducted via *in vivo* screening tests based on the seizure type rather than the etiology.

Evidently, the anticonvulsant activity is mainly due to the presence of the aryl binding site with aryl/alkyl hydrophobic group, hydrogen bonding domain, and electron donor group. These groups are the crucial requirements for the molecules to show potential action [12-15].

Encouraged by the promising pharmaceutical profiles of imidazoles and hydantoin as potent anticonvulsant entities [16-18], and in the continuation of our efforts [19, 20], new anticonvulsant compounds were prepared to look for safer, more selective and more effective candidates. In this study, two series of compounds as a hybrid structure from phenytoin and valproic acid were designed. The side chain was selected to mimic the length and lipophilic nature of valproic acid. Two series of imidazolidinediones and imidazoles were designed, synthesized, structurally characterized, and evaluated for the anticonvulsant and neurotoxic activities. Also, similarity to known drugs (phenytoin and valproic acid) was studied using ROCS (Rapid Overlay of Chemical Structure) technique. Moreover, physicochemical properties for final compounds were estimated to assess if these compounds possess drug-likeness properties or not.

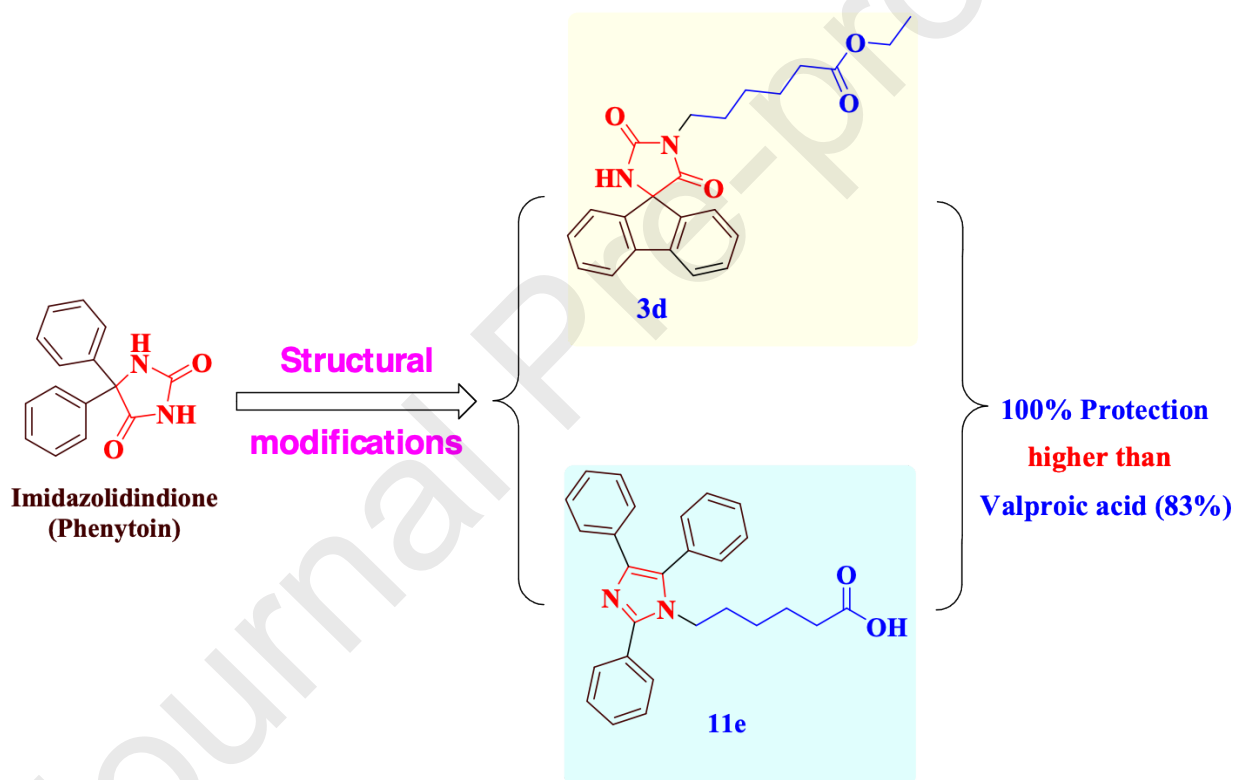
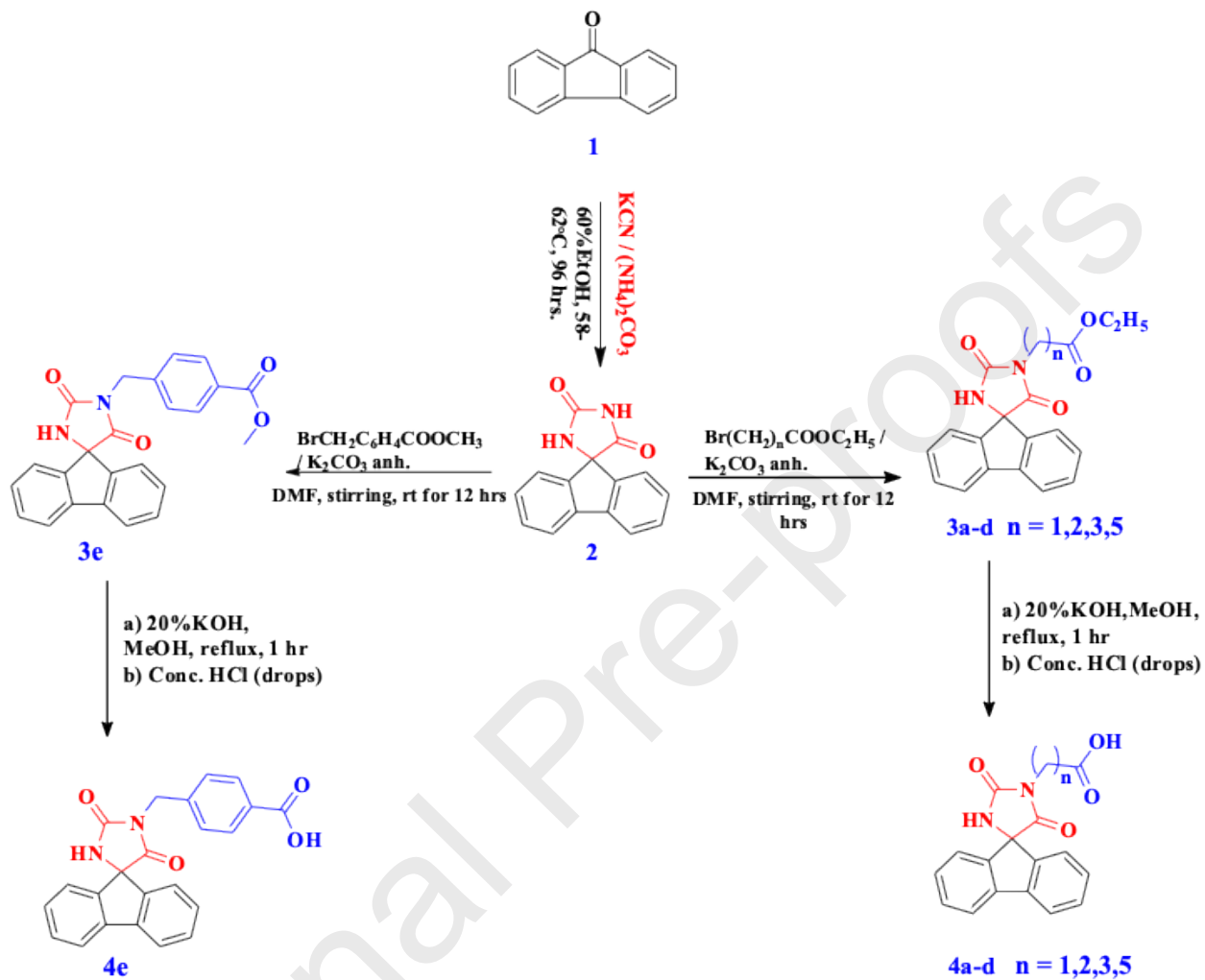


Figure1. The design strategy of novel phenytoin-valproic acid analogs

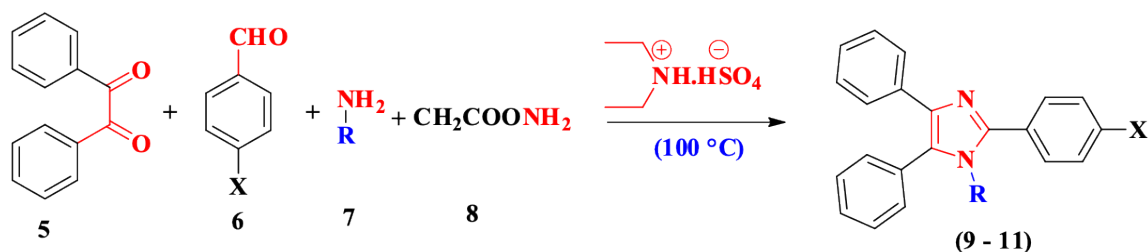
2. Results and Discussion

2.1 Synthesis

Sequential processes were done for the synthesis of the new compounds of imidazolidinedione and tetra-substituted imidazole derivatives (Schemes 1 and 2).



Scheme 1: Synthesis of imidazolidinedione derivatives (3a-e) and (4a-e).



Where X = OCH₃ (Series III) (9a - e)
 Cl (Series IV) (10a - e),
 H (Series V) (11a - e).

R =

- (a) -C₆H₅COOH
- (b) -CH₂CH₂COOH
- (c) -CH₂CH₂CH₂COOH
- (d) -CH₂CH₂CH₂CH₂COOH
- (e) -CH₂CH₂CH₂CH₂CH₂COOH

Scheme 2: Synthesis of multi-substituted imidazoles derivatives (9a-e), (10a-e) and (11a-e).

Imidazolidinediones (hydantoin)s (**3a-e**) were prepared in good yield by alkylation of the parent spiro hydantoin (spiro[fluorene-9,4'-imidazolidine]-2',5'-dione) **2** by heating of 9-fluorenone **1** with potassium cyanide and anhydrous ammonium carbonate as guided by Bucherer-Bergs reaction while following the method described by Nagasawa *et al* [21, 22]. This alkylation was done using methyl 4-bromomethyl benzoate, ethyl bromoacetate, ethyl 3-bromopropanoate, ethyl 4-bromobutyrate, or ethyl 6-bromohexanoate, in DMF and anhydrous K₂CO₃ to form the corresponding compounds (**3a-e**). The alkylation step was followed by a hydrolysis step which resulted in compounds (4a-e) with good yield (**Scheme 1**).

IR spectra of compounds **3a-e** showed significant stretching broad bands due to imidic NH groups at 3399-3174 cm⁻¹, three sharp stretching bands due to three carbonyl groups; two imidic and one ester moiety at 1778-1620 cm⁻¹. ¹H-NMR spectra of compounds **3a-d** showed the ethyl ester protons as a triplet integrated signal for methyl group (CH₂CH₃) from δ 1.20-1.16 ppm and a quartet at δ 4.05 ppm (CH₂CH₃). For compound **3e**, a singlet integrated signal for methyl group protons at δ 3.87 ppm and a singlet signal for 2 protons of CH₂ between N and the phenyl moiety at δ 4.79 ppm appeared. The amidic NH proton appeared as a singlet at δ 9.03-8.90 ppm, while both the aromatic moieties and aliphatic chains exhibited their signals at the expected δ values. ¹³C-NMR spectra of compounds **3a-d** showed signals for the ethyl ester carbons at approximately δ 14.43-14.60 ppm (upward in DEPT) corresponding to CH₃ group and at δ 60.37-61.96 ppm (downward in DEPT) corresponding to CH₂. Compound (**3e**); the methyl ester carbon appeared at

δ 52.64 ppm (upward in DEPT) and the carbon of CH₂ between N and the phenyl moiety appeared at δ 42.10 ppm (downward in DEPT). Spiro carbon in all compounds appeared at δ 77.56 ppm and absent in DEPT.

IR spectra for compounds **4a-e** showed significant stretching broad peaks at 3476-2563 cm⁻¹ due to hydroxyl group of carboxylic acid and three sharp intense stretching bands at 1775-1620 cm⁻¹ due to the three carbonyl groups; two imidic and one carboxylic carbonyl. ¹H-NMR spectra confirmed the absence of the ester protons in addition to the appearance of broad singlet peak at δ 12.36-11.94 ppm due to the carboxylic proton and a singlet peak at δ 8.84-8.82 ppm due to amidic NH proton. The aromatic and aliphatic moieties exhibited their proton signals at the expected δ values. ¹³C-NMR and DEPT spectra of compounds **4a-e** confirmed the absence of ester carbons. The imidazoles (**9a-e**), (**10a-e**) and (**11a-e**), [ϵ -(2-(substituted phenyl derivatives)-4,5-diphenyl-1H-imidazol-1-yl)alkanoic acids], were obtained in a high yield by reaction of benzil, aromatic aldehyde, amino acids (with a various spacer between the amino and carboxylic groups) and ammonium acetate by adding the catalytic efficiency of the ionic liquid, diethyl ammonium hydrogen sulfate (DEAHS) (**Scheme 2**). The reaction was found to be more facile under solvent-free conditions with higher yield and relatively in a very short time (35 minutes) [23-26].

IR spectra of compounds **9a-e**, **10a-e** & **11a-e** showed significant stretching broad bands due to carboxylic hydroxyl groups at 3400-2766 cm⁻¹, one sharp intense stretching band at 1607-1601 cm⁻¹ due to (C=N) group and one carbonyl of the carboxylic group at 1732-1675 cm⁻¹. In ¹H-NMR; the aromatic and the aliphatic protons moieties exhibited their proton signals at the expected δ values. In the case of (**9a-e**), ¹H-NMR spectra of compounds **9a-e** showed singlet signal at 3.93-3.74 ppm due to methoxy group. ¹³C-NMR and DEPT spectra of all compounds showed a signal at δ 169.42-178.55 ppm (absence in DEPT) indicates carbon of carboxylic carbonyl group. Compounds **9b-e**, **10b-e** and **11b-e** ¹³C-NMR and DEPT spectra confirmed the presence of an aliphatic side chain attached to N of imidazole by significant signals at δ 44.33-44.55 ppm (downward in DEPT). In the case of (**9a-e**), ¹³C-NMR spectra of compounds **9a-e** showed the appearance of a signal at 55.65-55.74 ppm (upward in DEPT) corresponding to the carbon of methoxy group. The structure and purity of target compounds were also confirmed by elemental analyses.

2.2. Anticonvulsant and neurotoxicity screening

The anticonvulsant activity and neurotoxicity of the target imidazolidinedione derivatives (**3a-e**) and (**4a-e**) and imidazole derivatives (**9a-e**), (**10a-e**) and (**11a-e**) are given in **Tables 1-4**. Two primary anticonvulsant screening models; MES and s.c. PTZ were performed in mice at a dose of 100 mg/kg. Diphenylhydantoin sodium and valproate sodium were used as reference standards for MES and PTZ, respectively. The neurotoxicity screening (rotarod test) was performed in mice at a dose of 100 mg/kg. Furthermore, the most active compounds were evaluated at different doses for determining the ED₅₀ of their anticonvulsant and neurotoxic activities [27].

2.2.1. Maximal electroshock seizure (MES) test.

The target compounds showed lesser protection against seizures than that of reference standard phenytoin. Compounds (**3a**, **3b**, **3d**, **4c**, and **4e**) were found to be effective with protection percentage (16.66, 33.33, 33.33, 16.66, 33.33%) respectively, on the other hand, imidazole series (**9a-e**), (**10a-e**) and (**11a-e**) were found inactive in this test, however, it was observed that most of the imidazole compounds showed variable protection in mice from mortality against the effect of MES induced seizures (Table 1).

Table 1: The anticonvulsant activity and percentage mortality prevention of the target compounds against MES induced seizures in mice in comparison with phenytoin.

Compound	Dose		Electric shock protection (%)	Mortality prevention (%)
	mg/kg	mmol/kg		
2	100	0.400	50	100
3a	100	0.295	16.66	66.66
3b	100	0.285	33.33	33.33
3c	100	0.274	0.00	100
3d	100	0.255	33.33	100
3e	100	0.251	0.00	100
4a	100	0.324	0.00	100
4b	100	0.310	0.00	33.33
4c	100	0.297	16.66	33.33
4d	100	0.274	0.00	100
4e	100	0.260	33.33	66.66
9a	100	0.224	0.00	100
9b	100	0.250	0.00	50
9c	100	0.242	0.00	50
9d	100	0.234	0.00	66.66
9e	100	0.227	0.00	66.66
10a	100	0.222	0.00	100

10b	100	0.248	0.00	100
10c	100	0.240	0.00	100
10d	100	0.232	0.00	100
10e	100	0.225	0.00	100
11a	100	0.240	0.00	100
11b	100	0.271	0.00	33.33
11c	100	0.261	0.00	33.33
11d	100	0.252	0.00	33.33
11e	100	0.243	0.00	66.66
Control	0	0	0	0
Phenytoin	100	0.396	100	100

2.2.2 Subcutaneous pentylenetetrazole (s.c. PTZ) test.

The initial anticonvulsant evaluation indicated that all compounds were effective in s.c. PTZ screening. In the imidazolidinedione series I (**3a-e**), compound **3d** showed complete protection (100%) against s.c. PTZ induced seizures illustrating higher potency than valproate sodium reference drug, which only achieved 83.33% protection at the same dosage level. Meanwhile, compound **3b** exhibited maximum protection of 83.33% as valproate sodium reference drug. Compound **3d** showed ED₅₀ of 55 mg/kg (Table 3). The results of all compounds of series I (**3a-e**) showed the anticonvulsant potential in the following decreasing order **3d** > **3b=2** > **3e** > **3c** > **3a**.

The results of series I (**3a-e**) against s.c. PTZ induced seizures showed that aliphatic substitution on N¹ with short-chain (**3a**) decreases the activity. But substitution with long aliphatic chain increased the anticonvulsant activity (maybe due to the increase in lipophilicity) and exceeded the anticonvulsant activity of unsubstituted parent compound (**2**) with exception to compound (**3c**). Also, when the aliphatic chain decreases with phenyl moiety (**3e**) (restricted free rotation), no change in the activity was found.

In the Imidazolidinediones series II (**4a-e**), compound **4e** showed complete protection (100%) against s.c. PTZ induced seizures compared to the reference drug valproate sodium, which achieved 83.33% protection at the same dose level. Meanwhile, compound **4c** exhibited maximum protection of 83.33% as valproate sodium. Also, the potency of compound **4e** was assured by ED₅₀ of 60 mg/kg, (Table 3). The members of series **4a-e** showed the anticonvulsant activity in the following decreasing order: **4e** > **4c=2** > **4b** = **4d** > **4a**.

The results from series II (**4a-e**) data also showed that by increasing the aliphatic side chain length (lipophilicity and partition coefficient) by the substitution on N¹, the anticonvulsant activity

increased against s.c. PTZ induced seizures till a certain length after which increase the length decreases the activity (parabolic relationship). Also, when part of the aliphatic chain was replaced with phenyl moiety (**4e**), which restricts free rotation, the activity increased.

By comparing the anticonvulsant activity of (**3a-e**) to (**4a-e**), it was found that the ester compounds were more active than that of carboxylic compounds which could be due to decreased lipophilicity affecting the crossing of the blood-brain barrier.

In the imidazoles (**9a-e**), (**10a-e**), and (**11a-e**), only compound **9d** emerged as the most potent member in the series (**9a-e**) as it displayed 83% protection against s.c. PTZ induced seizures as valproate sodium reference drug, and compounds **9a-e** showed the anticonvulsant potential in the following decreasing order: **9d** > **9a** > **4b** = **4c** = **9e**. While compound **10e** emerged as the most potent member in the series (**10a-e**), it displayed 83% protection against s.c. PTZ induced seizures compared to the reference drug valproate sodium. Series **10a-e** showed the anticonvulsant potential in the following decreasing order: **10e** > **10a** = **10b** > **10c** > **10d**. Compounds **11b** and **11e** displayed complete protection (100%) against s.c. PTZ induced seizures compared to valproate sodium, the reference drug, which achieved 83.33% protection at the same dose level. Meanwhile, compound **11a** exhibited maximum protection of 83.33% as valproate sodium reference drug. Compound **11b** showed ED₅₀ of 50 mg/kg. Series **10a-e** showed the anticonvulsant potential in the following decreasing order: **11b** > **11e** > **11a** > **11c** > **11d**. Furthermore, the resulted data from tetra substituted imidazole derivatives, series IV (**10a-e**) and series V (**11a-e**), showed that the longer the length of the aliphatic chain (N₁ substituted imidazole), the lower the anticonvulsant activity with the exception of **10e** and **11e**.

The carboxylic group on the side chain represents the HBD required for anticonvulsant activity. Thus, the length of this chain has two effects on anticonvulsant activity: an effect on the distance between the HBD and the structure of the whole molecule and an effect on lipophilicity (log p). When the aliphatic chain was replaced with phenyl moiety, an improvement was noticed in the anticonvulsant activity (**10a**) and (**11a**).

In conclusion, the three series [(**9a-e**), (**10a-e**) and (**11a-e**)] (with the exception of **d** members), which were substituted with an electron-withdrawing group (**Cl**), are more active than those substituted with an electron-donating group (**OCH₃**). On the other hand, the unsubstituted ones were more active than both the electron-withdrawing group (**Cl**) and the electron-donating group (**OCH₃**) (Table 2).

Table 2: Anticonvulsant activity of the target compounds against s.c. PTZ-induced seizures in comparison with valproate sodium.

Compound	Dose		PTZ- Protection (%)	Relative potency to standard
	mg/kg	mmol/kg		
2	100	0.400	83.33	100
3a	100	0.295	33.33	40.00
3b	100	0.285	83.33	100
3c	100	0.274	50.00	60.00
3d	100	0.255	100.00	120.00
3e	100	0.251	66.66	80.00
4a	100	0.324	16.67	20.00
4b	100	0.310	50.00	60.00
4c	100	0.297	83.33	100
4d	100	0.274	50.00	60.00
4e	100	0.260	100.00	120.00
9a	100	0.224	66.66	80.00
9b	100	0.250	50	60.00
9c	100	0.242	50	60.00
9d	100	0.234	83.33	100
9e	100	0.227	50	60.00
10a	100	0.222	66.66	80.00
10b	100	0.248	66.66	80.00
10c	100	0.240	50	60.00
10d	100	0.232	33.33	40.00
10e	100	0.225	83.33	100
11a	100	0.240	83.33	100
11b	100	0.271	100	120.00
11c	100	0.261	66.66	80.00
11d	100	0.252	16.66	20.00
11e	100	0.243	100	120.00
Control	0	0	0	0
Valproate sodium	100	0.602	83.33	100

The selected highest potent compounds (**3d**, **4e** and **11b**) from all series were subjected to the quantitative estimation (median effective dose, ED₅₀) through using different doses in s.c. PTZ induced seizures screening (Table 3).

Table 3: The median effective dose (ED₅₀) for compounds **3d**, **4e** and **11b** against s.c. PTZ induced seizures.

Compound	Dose (mg/kg)	PTZ-Protection	PTZ-Protection (%)	Mortality prevention (%)	Onset of convulsion per unprotected animal	ED ₅₀
3d	100	(6/6)	100	100		55
	80	(5/6)	83.33	83.33	after 6 min.	
	60	(3/6)	50	83.33	after 4, 8 & 23 min.	
	40	(2/6)	33.33	66.66	after 6, 10, 15 & 25 min.	
4e	100	(6/6)	100	100		60
	80	(5/6)	83.33	100	after 10 min.	
	60	(4/6)	66.66	83.33	after 6 & 8 min.	
	40	(1/6)	16.67	83.33	after 8, 10, 12, 18 & 2 min.	
11b	100	(6/6)	100	100		50
	80	(4/6)	66.66	100	after 10 & 14 min.	
	60	(4/6)	66.66	83.33	after 10 & 23 min.	
	40	(3/6)	50	50	after 5, 11 & 15 min.	
	20	(2/6)	33.33	50	after 8, 12, 15 & 15 min.	

2.2.3. Neurotoxicity screening (rotarod test):

The neurotoxicity screening (rotarod test) was performed in mice at a dose of 100 mg/kg. The results indicated that the ester compounds, as in series I (**3a-e**), increased the neurotoxicity. While carboxylic acid derivatives, as in series II (**4a-e**), decreased or prevented neurotoxicity. These findings motivated us to prepare carboxylic acid derivatives instead of ester derivatives as in series III (**9a-e**), series IV (**10a-e**), and series V (**11a-e**), whose neurotoxicity screening was dramatically abolished (Table 4) [28].

Table 4: Neurotoxicity (Rotarod test) screening data of (**3a-e**), (**4a-e**), (**9a-e**), (**10a-e**) and (**11a-e**) in mice with comparison to that of phenytoin.

Cmpd	Neurotoxicity	Neurotoxicity%	Cmpd	Neurotoxicity	Neurotoxicity%
2	(4/6)	66.66	9d	(3/6)	50
3a	(6/6)	100	9e	(6/6)	100
3b	(6/6)	100	10a	(0/6)	0
3c	(6/6)	100	10b	(0/6)	0
3d	(5/6)	83.33	10c	(0/6)	0
3e	(5/6)	83.33	10d	(0/6)	0
4a	(0/6)	0	10e	(0/6)	0
4b	(0/6)	0	11a	(0/6)	0
4c	(0/6)	0	11b	(0/6)	0
4d	(0/6)	0	11c	(0/6)	0

4e	(0/6)	0	11d	(0/6)	0
9a	(0/6)	0	11e	(0/6)	0
9b	(0/6)	0	Control	(0/6)	0
9c	(0/6)	0	Phenytoin	(3/6)	50

2.2.4. Cytotoxicity studies

The selected highest potent compounds (3d, 4e and 11b) from all the series were subjected to the quantitative estimation (median toxic dose eliciting minimal neurological toxicity in 50% of animals and the dose calculated in mg/kg, TD₅₀) through different doses (Table 5).

Table 5: Cytotoxicity studies for compounds (3d, 4e and 11b).

Compound	ED₅₀(S-PTZ, mg/kg)	LD₅₀ (mg/kg)	PI
3d	55	630	11.45
4e	60	622	10.3
11b	50	610	12.2

ED₅₀= median effective dose in 50% of animals

LD₅₀= median toxic dose eliciting minimal neurological toxicity in 50% of animals

PI= protective index (TD₅₀/ED₅₀)

2.3. Molecular modeling and Insilco study

2.3.1. ROCS application

ROCS is a virtual screening application used to perceive the similarity between chemical compounds based on their three-dimensional shape (3D)[29-31]. The 3D chemical shape represented good neighboring behavior, in which high similarity in shape reflects the high similarity in biology where the high similarity in biology is not reflected in the similarity in structure. ROCS technique has different applications including lead-hopping, molecular alignment, pose generation, and structural predictions[29].

The approach of this implemented work was to explain the activity of the compounds based on their 3D structures similarity to reported drug candidate (the query) and subsequently increase the chance of “scaffold hopping” or “lead hopping”.

ROCS alignment requires a) query molecules and here are phenytoin and valproic acid standard drugs, and b) the database molecules that our final compounds. The quality of alignment between query and the database was estimated using Tanimoto Combo (TC) scores [32]. Applying ROCS shape and color model for quires (phenytoin and valproic acid) was depicted in figures 2A and 2B, respectively. In the case of phenytoin, its shapes showed volume with 2 acceptors, 2 donors, and 3 rings, as in Figure 2A. Similarly, in the case of valproic acid, it adopted the shape with 2 acceptors, 1 donor, and 3 hydrophobic species, as depicted in Figure 2B. The structures of valproic

acid and phenytoin, as presented in figure 2C, overlaid and perceived TC scores of 0.7, as shown in Table 6.

2.3.2. ROCS study using valproic acid as a query:

Both hydantoin derivatives (series **a**) and imidazole derivatives (series **b**) aligned and overlaid with the valproic acid query shape with lower TC scores in comparison to phenytoin, as in the query Table 5. Compound **3d**, with TS 0.51, as an example of hydantoin series, overlaid with valproic acid and its butyl side chain which occupies the hydrophobic color of valproic acid as shown in Figure 4A. The compound **4e**, with TS 0.44, adopted different poses with valproic acid, but the benzyl side chain located outside the volume, as illustrated in Figure 4B. In the case of the imidazole series, it adopted dissimilarity with valproic acid shape. As shown in Figure 4C, compound **11e** exhibited dissimilarity with valproic acid with Tanimoto score 0.52, as in Table 6.

Table 6: Tanimoto Combo scores for all compounds in comparison to phenytoin and valproic acid.

		Tanimoto Combo Scores, Phenytoin as query	Tanimoto Combo Scores, Valproic acid as query
	Phenytoin	2	0.704
	Valproic	0.73	2
1	3a	1.2	0.53
2	10c	0.71	0.53
3	4c	1.14	0.52
4	4a	1.2	0.52
5	4b	1.16	0.54
6	10e	0.717	0.52
7	11b	0.713	0.52
8	3b	1.2	0.51
9	10b	0.70	0.51
10	3d	1.12	0.51
11	4d	1.07	0.50
12	11c	0.69	0.50
13	3c	1.20	0.50
14	11e	0.72	0.50
15	9e	0.69	0.49
16	9c	0.68	0.49
17	9b	0.69	0.48
18	10d	0.76	0.47
19	9d	0.72	0.45
20	4e	1.01	0.44
21	11d	0.75	0.44
22	3e	1.08	0.42
23	11a	0.716	0.37
24	10a	0.70	0.36
25	9a	0.68	0.35

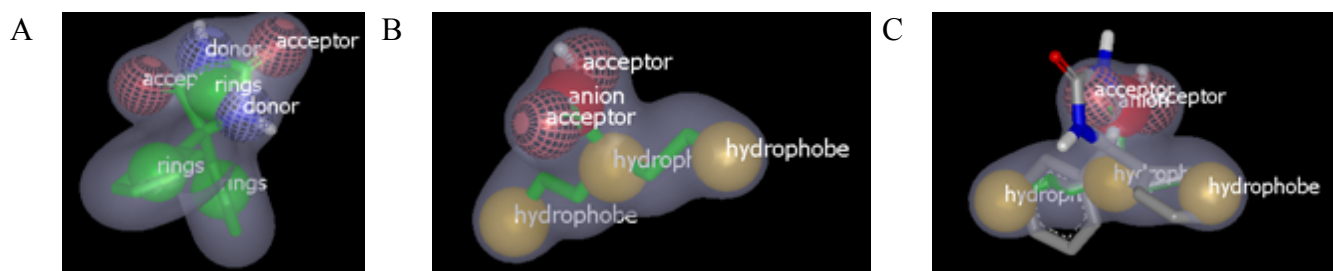


Figure 2: vROCS representation shape and color atoms of: A) Phenytoin B) Valproic acid by vROCS application; C) Overlay and alignment valproic acid on phenytoin.

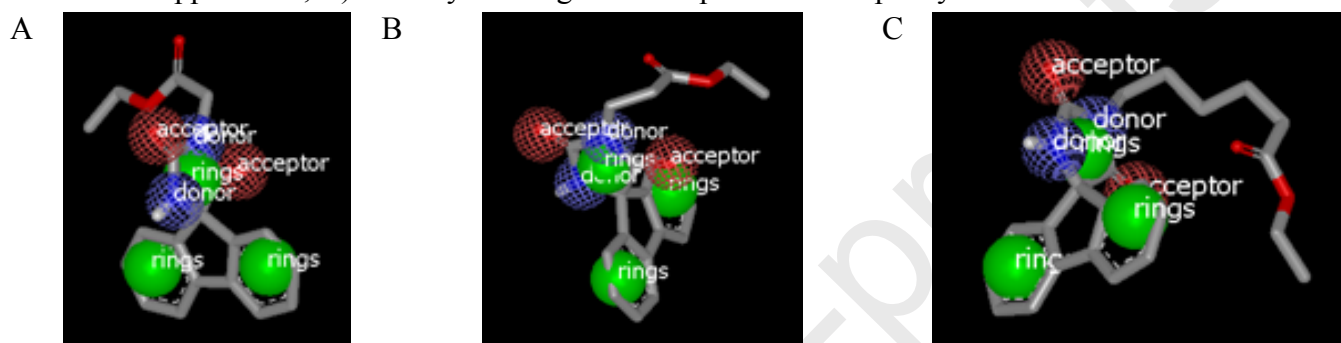


Figure 3: A) Representation shape and color of **3a** using phenytoin as query by vROCS application; B) Representation shape and color of **3b** using phenytoin as query by vROCS application; C) Representation shape and color of **3d** using phenytoin as query by vROCS application.

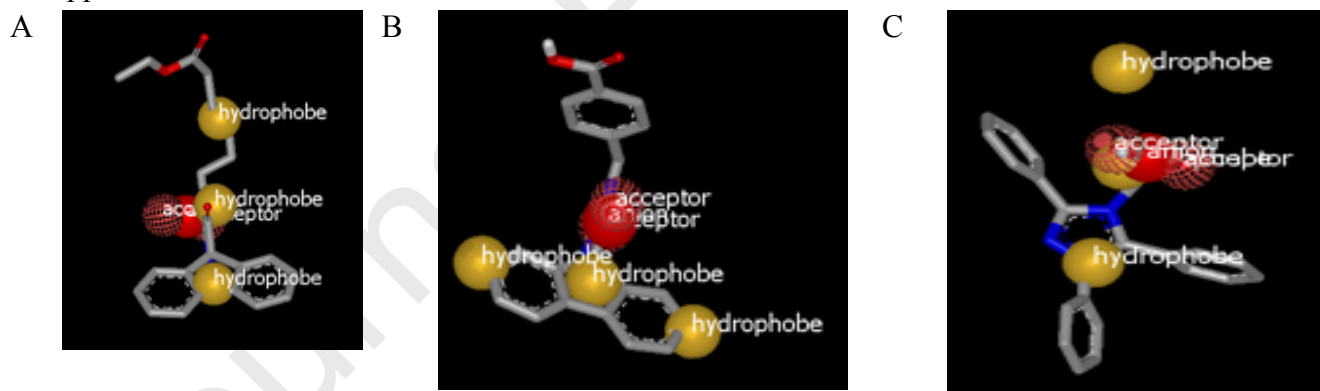


Figure 4: A) Representation shape and color of **3d** using valproic acid as query by vROCS application; B) Representation shape and color of **4e** using valproic acid as query by vROCS application; C) Representation shape and color of **11b** using valproic acid as query by vROCS application.

Based on ROCS visualization and TC scores, these compounds have high similarity to hydantoin. In compounds with the general formula of **series a**, the 9H-fluorene moiety illustrated color and shape similarity for both hydantoin and valproic acid. These results will guide us to move forward in the development of new anticonvulsant candidate that have general formula from **series a**.

II.3.3. In silico prediction of pharmacokinetics and pharmacodynamics parameters and drug-likeness data for the active compounds:

Over the **past** few decades, **scientists found** that some bioactive molecules cannot be prioritized as a good drug candidate due to limited bioavailability[7]. About 30% of oral drug subjected to stopping their process in drug development and manufacturing due to poor pharmacokinetics. Thus, an in-silico model for predicting oral bioavailability is very important to **picking** the most promising compounds for further optimization and clinical development[8].

In the present study, the final compounds were subjected to molecular properties prediction and drug-likeness by Molinspiration & Mol-Soft, and Preadmet software [33-35].

Table 6 contains the calculated topological molecular polar surface area (TPSA) for the investigated compounds. All compounds have TPSA in the region of 37.3-86.7. It is known that for molecules to penetrate the blood–brain barrier (BB), a PSA should be less than 90 angstroms squared and TPSA values, for most known drugs, have to be below 140-150 Å² [9, 10].

Compounds 11b, 11c, 10b, 9b, and 9c have BBB values of 5.23-1.13, which are higher than both standard drugs, phenytoin and valproic acid (BBB = 0.9). Compounds **9d** and **11d** have BBB values 0.65 and 0.53 respectively. All other compounds have lower BBB in comparison to standard drugs used here.

In general, the compounds in the present study possess a high number of rotatable bonds (NRT), 2-9, except compound **9e**, which has 10 NRT as shown in Table 6. Therefore, these compounds exhibit large conformational flexibility. In addition, all compounds obey Lipinski's rule of five except compounds **9d**, **9e**, **10b**, **10c**, **10e**, and **11e** have higher log *p* (5.6-6.9).

The drug-likeness model score is defined as a combined effect of physicochemical properties, pharmacodynamics and pharmacokinetics of a compound and it is represented by a numerical value[11]. Compounds with zero or negative value could not be considered as drug-like. In this study, 12 compounds acquired drug-likeness scores from 0.14-0.79, while other compounds showed negative values in comparison to phenytoin and valproic acids (12-20) respectively), table 6.

Plasma protein binding (PPB) and percentages of human intestinal absorption (HIA) were calculated as examples of pharmacokinetic parameters. All compounds exhibited high PPB values (more than 86) except compounds **4c**, and **3c**, which had low values (54, 63 respectively). Regarding HIA, all compounds showed high values.

Table 7: Predicted of pharmacokinetic and pharmacodynamic parameters compounds and standard drugs

Compound	Lipniski rule of five					TPSA	No. violations	Drug-likeness model score	BBB	PPB	HIA
	Mwt	NRB	HBA	HBD	LogP						
Phenytoin	252.27	2	2	2	2.18	58.20	0	0.12	0.92	96.58	92.53
Valproic	144.21	5	2	1	2.80	37.30	0	0.20	0.91	100.00	93.71
1 3a	336.35	4	5	1	2.15	75.71	0	-1.43	0.05	86.30	96.44
2 10c	416.91	7	3	1	5.72	55.12	1	0.79	0.44	100.00	97.62
3 4c	336.35	4	4	2	2.15	86.71	0	-0.83	0.26	54.62	96.27
4 4a	308.29	2	4	2	0.69	86.71	0	-1.02	0.36	90.58	95.32
5 4b	322.32	3	4	2	1.88	86.71	0	-0.95	0.36	92.58	95.85
6 10e	444.96	9	3	1	6.93	55.12	1	0.83	0.21	100.00	97.73
7 11b	368.44	6	3	1	4.97	55.12	1	-0.12	5.25	92.94	97.39
8 3b	350.37	5	4	1	2.56	75.71	1	-1.30	0.16	94.23	96.52
9 10b	402.88	6	3	1	5.65	55.12	1	0.66	2.10	100.00	97.57
10 3d	392.45	8	4	1	3.84	75.71	0	-1.09	0.04	87.27	96.41
11 4d	364.40	6	4	2	3.16	86.71	0	-0.79	0.026	86.19	96.86
12 11c	382.46	7	3	1	5.24	55.12	1	0.10	3.12	98.06	97.41
13 3c	364.40	6	4	1	2.83	75.71	0	-1.13	0.13	63.38	96.50
14 11e	410.52	9	3	1	6.25	55.12	1	0.14	0.13	100.00	97.49
15 9e	440.54	10	4	1	6.31	64.36	1	0.39	0.19	97.86	97.46
16 9c	412.49	8	4	1	5.30	64.36	1	0.32	1.13	94.88	97.46
17 9b	398.46	7	4	1	5.03	64.36	1	0.18	2.82	91.48	97.48
18 10d	430.94	8	3	1	6.43	55.12	1	0.83	0.36	100.00	97.68
19 9d	426.52	9	4	1	5.80	64.36	1	0.39	0.65	96.20	97.45
20 4e	384.39	3	4	2	3.67	86.71	0	-0.06	0.36	97.73	97.08
21 11d	396.49	8	3	1	5.75	55.12	1	0.14	0.53	99.52	97.45
22 9a	446.51	6	4	1	6.70	64.36	1	-0.97	0.23	100.00	97.64
23 3e	398.42	4	3	1	3.93	75.71	0	0.53	0.10	96.32	96.31
24 10a	450.93	5	3	1	7.32	55.12	1	-0.58	0.40	100.00	97.97
25 11a	416.48	5	3	1	6.64	55.12	1	-0.94	0.43	100.00	97.73

LogP: logarithm of compound partition coefficient between n-octanol and water.

M.Wt: molecular weight.

HBA: number of hydrogen bond acceptors.

HBD: number of hydrogen bond donors.

HBA: number of hydrogen bond acceptors.

TPSA: polar surface area.

BBB: Blood Brain Barrier.

PPB: plasma protein binding

NRB: number of rotation bonds.

HIA: Percentages of human intestinal absorption

To conclude, results showed that the most active compounds exhibited reasonable physicochemical properties with good predicted drug-likeness values, which might elevate them to be drug candidates.

2.4. Conclusion:

A group of new imidazolidinedione and tetra-substituted imidazole derivatives were synthesized and characterized by their spectral data. They were compromised in two series: imidazolidinedione (**3a-e**), (**4a-e**), and imidazole derivatives (**9a-e**), (**10a-e**) and (**11a-e**). These compounds showed from promising to moderate anticonvulsant activities. The obtained results revealed that compound (**3d**), which has a longer aliphatic side chain (n=5) linked to the imidazolidinedione nucleolus, showed complete protection (100%) against s.c. PTZ induced seizures compared to valproate sodium reference drug, which achieved 83.33% protection at the same dose level. Also, compound (**4e**), which has methyl benzoic acid moiety linked to the imidazolidinedione, exhibited complete protection (100%) against s.c. PTZ induced seizures. On the other hand, imidazole compounds as 3-(2,4,5-triphenyl-1H-imidazol-1-yl)propanoic acid (**11b**) and 5-(2,4,5-triphenyl-1H-imidazol-1-yl)pentanoic acid (**11e**) exhibited complete protection (100%) against s.c. PTZ induced seizures. The neurotoxicity screening showed the absence of toxic effects at the tested dose level for all series, which has a free carboxylic group. Moreover, the neurotoxicity increased after replacing the carboxylic group by ester moiety as in series II that may be due to the increasing in the hydrophilic properties of the compounds. Finally, it was found that these compounds could decrease the threshold of seizures rather than the prevention of their spread. This was concluded from their anticonvulsant activity against s.c. PTZ induced seizures and inactivity of these compounds against the MES test. Furthermore, these active compounds may be valuable in the treatment of petit mal seizures more than grand mal seizures as (**4e**), (**3d**), (**11b**) and (**11e**) revealed promising anticonvulsant agents. Shape similarity study and physicochemical calculations advocates future work with potent and safe anticonvulsant drugs.

3. Experimental

Stuart electro-thermal melting point equipment was used for melting points determination and was uncorrected. Nicolet iS5 FT-IR spectrometer was used for recording IR spectra while a Bruker Advance 400 MHz NMR spectrometer was used for recording NMR spectra, using TMS as an internal reference, at Sohag University, Egypt. Chemical shifts (δ) values were given in parts per million (ppm) relative to CDCl_3 (7.29 for proton and 76.9 for carbon) or $\text{DMSO}-d_6$ (2.50 for proton and 39.50 for carbon) and

coupling constants (J) in Hertz. Vario El Elementar CHN Elemental analyzer in the Regional Center for Mycology and Biotechnology, Naser City, Cairo, Egypt was used for elemental analysis and the results were within $\pm 0.4\%$ of the theoretical values. Thin-layer chromatography (TLC) using Merck 9385 pre-coated aluminum plate silica gel (Kieselgel 60) 5 x 20 cm plates with a layer thickness of 0.2 mm were used for monitoring the progress of reactions and the purity of the prepared compounds. All solvents were dried by standard methods. 9-fluorenone **1** and methyl 4-bromomethyl benzoate were purchased from Sigma Aldrich, other materials and solvent used in the preparation of intermediate and target compounds were purchased from El-Nasr pharmaceutical chemicals company, Egypt.

3.1. Synthesis of Spiro[fluorene-9,4'-imidazolidine]-2',5'-dione (**2**)

The Spiro[fluorene-9,4'-imidazolidine]-2',5'-dione (**2**) was synthesized as reported[22] giving dark yellow to brown crystals (92% yield) mp.353 °C, reported more than 300 °C.

3.1.1. General procedure for synthesis of ethyl ϵ -(2',5'-dioxospiro[fluorene-9,4'-imidazolidine]-1'-yl)alkanoate (**3a-d**) and methyl 4-((2',5'-dioxospiro[fluorene-9,4'-imidazolidine]-1'-yl)methyl)benzoate (**3e**)

A mixture of the imidazolidinedione **2** (1.251 g, 5 mmol), (**5.5** mmol) of an appropriate ester [methyl 4-bromomethyl benzoate (1.259 g), ethyl bromoacetate (0.918 g), ethyl 3-bromopropanoate (0.995 g), ethyl 4-bromobutyrate (1.073 g), ethyl 6-bromohexanoate (1.228 g) and anhydrous potassium carbonate (1.382 g, 10 mmol) in DMF (20 mL) was allowed to stir at room temperature for 12 hrs. The reaction mixture was diluted with ice water and the resulting precipitate was filtered, washed with water and dried. The crude product was purified by crystallization from aqueous ethanol to form the corresponding compound (**3a-e**).

Methyl 4-((2', 5'-dioxospiro[fluorene-9,4'-imidazolidine]-1'-yl)methyl)benzoate (**3e**):

Reaction of **2** with methyl 4-bromomethylbenzoate, white powder; Yield (98%); mp. 248-250 °C; IR (cm^{-1}): 3307 (NH), 1772 (C=O), 1710 (C=O), 1611 (C=O), 1104 (C-O); $^1\text{H-NMR}$ (400 MHz, $\text{DMSO-}d_6$) δ (ppm): 4.79 (s, 2H, N-CH₂), 3.87 (s, 3H, O-CH₃), 7.38 (d, 2H, $J = 8.00$ Hz, 2 Ar-H), 7.47 (t, 2H, $J = 8.00$ Hz, 2 Ar-H), 7.50 (d, 2H, $J = 8.00$ Hz, 2 Ar-H), 7.51 (d, 2H, $J = 8.00$ Hz, 2 Ar-H), 8.01 (d, 2H, $J = 8.00$ Hz, 2 Ar-H), 8.03 (d, 2H, $J = 8.00$ Hz, 2 Ar-H), 9.11 (s, 1H, NH); $^{13}\text{C-NMR}$ (100 MHz, $\text{DMSO-}d_6$) δ (ppm): 42.10 (CH₂), 52.64 (OCH₃), 71.56 (C(spiro)), 121.24, 121.34, 124.10, 124.76, 127.84, 127.99, 128.59, 128.94, 129.28, 130.13, 130.50, 130.80, 140.59, 141.17, 141.37, 142.50, 142.88, 157.02, 162.78, 166.43, 172.85; Elemental analysis for C₂₄H₁₈N₂O₄ (Calcd./Found); C, 72.35/72.57; H, 4.55/4.58; N, 7.03/7.11.

Ethyl 2-(2',5'-dioxospiro[fluorene-9,4'-imidazolidine]-1'-yl)acetate 3a:

Reaction of **2** with ethyl bromoacetate; white powder (yield 90%); mp. (196) °C : IR (cm⁻¹): 3399 (NH), 1770 (C=O), 1734 (C=O), 1627 (C=O), 1145 (C-O); ¹H-NMR (400 MHz, DMSO-*d*₆) δ (ppm): 1.26 (t, 3H, *J* = 7.20 Hz, CH₂-CH₃), 4.35 (s, 2H, N-CH₂), 4.22 (q, 2H, *J* = 7.20 Hz, O-CH₂-CH₃), 7.39 (d, 2H, *J* = 8.00 Hz, 2 Ar-H), 7.42 (t, 2H, *J* = 8.00 Hz, 2 Ar-H), 7.51 (d, 2H, *J* = 8.00 Hz, 2 Ar-H), 7.93 (d, 2H, *J* = 8.00 Hz, 2 Ar-H), 9.03 (s, 1H, NH); ¹³C-NMR (100 MHz, DMSO-*d*₆) δ (ppm): 14.47 (CH₃), 40.30 (CH₂), 61.96 (CH₂), 71.68 (C(spiro)), 121.26, 124.25, 125.31, 128.83, 130.50, 131.13, 139.39, 141.21, 141.88, 142.89, 155.52, 156.52, 162.76, 167.19, 172.61; Elemental analysis for C₁₉H₁₆N₂O₄ (Calcd./Found); C, 67.85/68.02; H, 4.79/4.86; N, 8.33/8.51.

Ethyl 3-(2',5'-dioxospiro[fluorene-9,4'-imidazolidine]-1'-yl)propanoate (3b): reaction of **2** with ethyl 3-bromopropionate; white powder (yield: 90%); mp. 178-180 °C; IR (cm⁻¹): 3174 (NH), 1774 (C=O), 1713 (C=O), 1618 (C=O), 1181 (C-O); ¹H NMR (400 MHz, DMSO-*d*₆) δ (ppm): 1.19 (t, 3H, *J* = 7.20 Hz, CH₂-CH₃), 2.68 (t, 2H, *J* = 6.80 Hz, CH₂-CO), 3.78 (t, 2H, *J* = 6.80 Hz, N-CH₂), 4.09 (q, 2H, *J* = 7.20 Hz, O-CH₂-CH₃), 7.37 (d, 2H, *J* = 8.00 Hz, 2 Ar-H), 7.48 (t, 2H, *J* = 8.00 Hz, 2 Ar-H), 7.51 (d, 2H, *J* = 8.00 Hz, 2 Ar-H), 7.93 (d, 2H, *J* = 8.00 Hz, 2 Ar-H), 8.9 (s, 1H, NH); ¹³C-NMR (100 MHz, DMSO-*d*₆) δ (ppm): 14.43 (CH₃), 32.71 (CH₂), 40.30 (NCH₂), 60.72 (OCH₂), 71.32 (C(spiro)), 121.18, 121.58, 124.19, 124.56, 128.74, 128.74, 130.37, 130.90, 140.54, 141.20, 141.67, 143.10, 156.43, 171.06, 172.68.; Elemental analysis for C₂₀H₁₈N₂O₄ (Calcd./Found); C, 68.56/68.79; H, 5.18/5.23; N, 8.00/8.23.

Ethyl 4-(2',5'-dioxospiro[fluorene-9,4'-imidazolidine]-1'-yl)butanoate (3c): Reaction of **2** with ethyl 4-bromobutyrate; white powder (yield 97%); mp. 145-150 °C: IR (cm⁻¹): 3330 (NH), 1779 (C=O), 1707 (C=O), 1680 (C=O), 1095 (C-O); ¹H-NMR (400 MHz, DMSO-*d*₆) δ (ppm): 1.19 (t, 3H, *J* = 7.20 Hz, CH₂-CH₃), 1.88-1.91 (m, 2H, CH₂-CH₂-CO), 2.40 (t, 2H, *J* = 6.80 Hz, CH₂-CO), 3.58 (t, 2H, *J* = 6.80 Hz, N-CH₂), 4.09 (q, 2H, *J* = 7.20 Hz, O-CH₂-CH₃), 7.37 (d, 2H, *J* = 8.00 Hz, 2 Ar-H), 7.48 (t, 2H, *J* = 8.00 Hz, 2 Ar-H), 7.52 (d, 2H, *J* = 8.00 Hz, 2 Ar-H), 7.94 (d, 2H, *J* = 8.00 Hz, 2 Ar-H), 8.95 (s, 1H, NH); ¹³C-NMR (100 MHz, DMSO-*d*₆) δ (ppm): 14.43 (CH₃), 23.52 (CH₂), 30.90 (CH₂), 40.30 (NCH₂), 60.37 (OCH₂), 71.40 (C(spiro)), 121.26, 121.56, 124.08, 124.48, 128.84, 130.40, 130.82, 140.86, 141.19, 141.65, 143.12, 157.37, 172.45, 172.71, 173.07.; Elemental analysis for C₂₁H₂₀N₂O₄ (Calcd./Found); C, 69.22/69.47; H, 5.53/5.59; N, 7.69/7.88.

Ethyl 6-(2',5'-dioxospiro[fluorene-9,4'-imidazolidine]-1'-yl)hexanoate (3d): reaction of **2** with ethyl 6-bromohexanoate; white powder (yield 86.7%); mp. 104-106 °C; IR (cm⁻¹): 3175 (NH),

1770 (C=O), 1703 (C=O), 1680 (C=O), 1098 (C-O); $^1\text{H-NMR}$ (400 MHz, DMSO- d_6) δ (ppm): 1.19 (t, 3H, $J = 7.20$ Hz, $\text{CH}_2\text{-CH}_3$), 1.34-1.35 (m, 2H, $\text{CH}_2\text{-CH}_2\text{-CO}$), 1.58-1.66 (m, 4H, $\text{CH}_2\text{-CH}_2\text{-CH}_2\text{-CH}_2\text{-CO}$), 2.32 (t, 2H, $J = 7.20$ Hz, $\text{CH}_2\text{-CO}$), 3.53 (t, 2H, $J = 7.20$ Hz, N- CH_2), 4.07 (q, 2H, $J = 7.20$ Hz, O- $\text{CH}_2\text{-CH}_3$), 7.37 (d, 2H, $J = 8.00$ Hz, 2 Ar-H), 7.45 (t, 2H, $J = 8.00$ Hz, 2 Ar-H), 7.52 (d, 2H, $J = 8.00$ Hz, 2 Ar-H), 7.94 (d, 2H, $J = 8.00$ Hz, 2 Ar-H), 8.93 (s, 1H, NH); $^{13}\text{C-NMR}$ (100 MHz, DMSO- d_6) δ (ppm): 14.60 (CH_3), 24.50 (CH_2), 26.01 (CH_2), 27.71 (CH_2), 33.79 (CH_2), 38.76 (N CH_2), 60.37 (O CH_2), 71.38 (C(spiro)), 121.28, 121.59, 123.98, 124.36, 128.79, 128.84, 130.38, 130.81, 140.80, 141.20, 141.80, 143.15, 157.42 (NCO), 172.96 (NCO), 173.28.; EI-MS (70 eV) m/z (%): 392 (28) (M^+), 347 (11), 305 (17), 291 (1), 264 (2), 206 (17), 192 (27), 179 (100), 140 (60); Elemental analysis for $\text{C}_{23}\text{H}_{24}\text{N}_2\text{O}_4$ (Calcd./Found); C, 70.39/70.51; H, 6.16/6.25; N, 7.14/7.32.

3.1.2. General procedure for the synthesis of ϵ -(2',5'-dioxospiro[fluorene-9,4'-imidazolidine]-1'-yl)alkanoic acids (4a-d) and 4-((2',5'-dioxospiro[fluorene-9,4'-imidazolidine]-1'-yl)methyl)benzoic acid (4e).

To (1 mmol) of an appropriate ester (3a-e) add 20 mL of 1N NaOH then stir at room temperature for 16 hrs. The reaction mixture was filtered off and the filtrate was cooled to 0 °C. Then the reaction mixture was acidified with hydrochloric acid. The obtained solid was separated, washed with water, dried and crystallized from ethanol.

4-((2',5'-Dioxospiro[fluorene-9,4'-imidazolidine]-1'-yl)methyl) benzoic acid (4e): white powder (88%); mp. 220-222 °C; IR (cm^{-1}): 3476-2641 (OH), 3290.83 (NH), 1775 (C=O), 1707 (C=O), 1612 (C=O), 1106 (C-O); $^1\text{H-NMR}$ (400 MHz, DMSO- d_6) δ (ppm): 4.80 (s, 2H, N- CH_2), 7.36 (d, 2H, $J = 8.00$ Hz, 2 Ar-H), 7.42 (t, 2H, $J = 8.00$ Hz, 2 Ar-H), 7.49 (d, 2H, $J = 8.00$ Hz, 2 Ar-H), 7.53 (d, 2H, $J = 8.00$ Hz, 2 Ar-H), 7.91 (d, 2H, $J = 8.00$ Hz, 2 Ar-H), 8.01 (d, 2H, $J = 8.00$ Hz, 2 Ar-H), 8.99 (s, 1H, NH), 12.59 (br s, 1H, OH); $^{13}\text{C-NMR}$ (100 MHz, DMSO- d_6) δ (ppm): 42.24 (CH_2), 71.67 (C(spiro)), 121.25, 121.34, 123.98, 124.66, 127.88, 127.99, 128.47, 128.87, 129.35, 130.21, 130.26, 130.43, 140.59, 141.22, 141.37, 142.50, 142.88, 143.02, 157.02, 166.43, 172.85; Elemental analysis for $\text{C}_{23}\text{H}_{16}\text{N}_2\text{O}_4$ (Calcd./Found); C, 71.87/72.05; H, 4.20/4.24; N, 7.29/7.38.

2-(2',5'-Dioxospiro[fluorene-9,4'-imidazolidine]-1'-yl)acetic acid (4a): white powder (yield 86%); mp. 212-215 °C; IR (cm^{-1}): 3070-2563 (OH), 3358 (NH), 1775 (C=O), 1705.71 (C=O), 1622 (C=O); $^1\text{H-NMR}$ (400 MHz, DMSO- d_6) δ (ppm): 4.24 (s, 2H, N- CH_2), 7.39 (d, 2H, $J = 8.00$

Hz, 2 Ar-H), 7.50 (t, 2H, $J = 8.00$ Hz, 2 Ar-H), 7.53 (d, 2H, $J = 8.00$ Hz, 2 Ar-H), 7.91 (d, 2H, $J = 8.00$ Hz, 2 Ar-H), 8.92 (s, 1H, **NH**), 13.19 (br s, 1H, **OH**); $^{13}\text{C-NMR}$ (100 MHz, $\text{DMSO-}d_6$) δ (ppm): 40.30 (CH_2), 71.68 (C(spiro)), 121.17, 124.26, 125.31, 128.77, 130.42, 131.13, 139.39, 141.23, 141.88, 143.05, 155.52, 156.52, 162.76, 167.19, 172.61; Elemental analysis for $\text{C}_{17}\text{H}_{12}\text{N}_2\text{O}_4$ (Calcd./Found); C, 70.39/70.60; H, 6.16/6.24; N, 7.14/7.19.

3-(2',5'-Dioxospiro[fluorene-9,4'-imidazolidine]-1'-yl)propanoic acid (4b): white powder (yield 80%); mp.185 °C; IR (cm^{-1}): 3200-2670 (OH), 3345 (NH), 1772 (C=O), 1700 (C=O), 1683 (C=O); $^1\text{H-NMR}$ (400 MHz, $\text{DMSO-}d_6$) δ (ppm): 2.67 (t, 2H, $J = 6.80$ Hz, **CH₂-CO**), 3.79 (t, 2H, $J = 6.80$ Hz, **N-CH₂**), 7.37 (d, 2H, $J = 8.00$, 2 Ar-H), 7.49 (t, 2H, $J = 8.00$ Hz, 2 Ar-H), 7.52 (d, 2H, $J = 8.00$ Hz, 2 Ar-H), 7.90 (d, 2H, $J = 8.00$ Hz, 2 Ar-H), 8.8 (s, 1H, **NH**), 11.89 (br s, 1H, **OH**); $^{13}\text{C-NMR}$ (100 MHz, $\text{DMSO-}d_6$) δ (ppm): 32.57 (CH_2), 40.30 (NCH_2), 71.38 (C(spiro)), 121.10, 121.58, 124.24, 125.56, 127.97, 128.66, 128.73, 130.30, 140.54, 141.23, 141.67, 143.22, 157.06, 172.53, 172.71.; Elemental analysis for $\text{C}_{18}\text{H}_{14}\text{N}_2\text{O}_4$ (Calcd./Found); C, 67.07/67.34; H, 4.38/4.36; N, 8.69/8.78.

4-(2',5'-Dioxospiro[fluorene-9,4'-imidazolidine]-1'-yl)butanoic acid (4c): white powder (yield 83%); mp.183 °C; IR ν (cm^{-1}): 3153-2629 (OH), 3340 (NH), 1766 (C=O), 1696 (C=O), 1620 (C=O); $^1\text{H-NMR}$ (400 MHz, $\text{DMSO-}d_6$) δ (ppm): 1.87-1.93 (m, 2H, **CH₂-CH₂-CO**), 2.32 (t, 2H, $J = 6.80$ Hz, **CH₂-CO**), 3.58 (t, 2H, $J = 6.80$ Hz, **N-CH₂**), 7.36 (d, 2H, $J = 8.00$ Hz, 2 Ar-H), 7.49 (t, 2H, $J = 8.00$ Hz, 2 Ar-H), 7.53 (d, 2H, $J = 8.00$ Hz, 2 Ar-H), 7.93 (d, 2H, $J = 8.00$ Hz, 2 Ar-H), 8.80 (s, 1H, **NH**), 12.11 (br s, 1H, **OH**); $^{13}\text{C-NMR}$ (100 MHz, $\text{DMSO-}d_6$) δ (ppm): 23.64 (CH_2), 31.43 (CH_2), 38.60 (NCH_2), 71.49 (C(spiro)), 121.26, 121.56, 124.08, 124.48, 128.77, 128.87, 130.40, 130.82, 141.22, 141.65, 143.24, 157.38, 172.45, 173.01, 174.08.; Elemental analysis for $\text{C}_{19}\text{H}_{16}\text{N}_2\text{O}_4$ (Calcd./Found): C, 67.85/68.09; H, 4.79/4.88; N, 8.33/8.51.

6-(2',5'-Dioxospiro[fluorene-9,4'-imidazolidine]-1'-yl)hexanoic acid (4d): yellowish white powder (yield 93%); mp.145-147 °C; IR (cm^{-1}): 3058-2864 (OH), 3393 (NH), 1775 (C=O), 1707 (C=O), 1689 (C=O); $^1\text{H-NMR}$ (400 MHz, $\text{DMSO-}d_6$) δ (ppm): 1.36-1.38 (m, 2H, **CH₂-CH₂-CH₂-CO**), 1.58-1.68 (m, 4H, **CH₂-CH₂-CH₂-CH₂-CO**), 2.25 (t, 2H, $J = 7.20$ Hz, **CH₂-CO**), 3.54 (t, 2H, $J = 7.20$ Hz, **N-CH₂**), 7.37 (d, 2H, $J = 8.00$ Hz, 2 Ar-H), 7.49 (t, 2H, $J = 8.00$ Hz, 2 Ar-H), 7.53 (d, 2H, $J = 8.00$ Hz, 2 Ar-H), 7.91 (d, 2H, $J = 8.00$ Hz, 2 Ar-H), 8.80 (s, 1H, **NH**), 11.94 (br s, 1H, **OH**); $^{13}\text{C-NMR}$ (100 MHz, $\text{DMSO-}d_6$) δ (ppm): 24.55 (CH_2), 26.16 (CH_2), 27.72 (CH_2), 34.00 (CH_2), 38.85 (NCH_2), 71.48 (C(spiro)), 121.28, 121.59, 123.98, 124.36, 128.79, 128.84, 130.38,

130.81, 140.80, 141.23, 141.80, 143.25, 157.44, 172.94, 174.69.; EI-MS (70 eV) m/z (%): 364 (1) (M⁺), 321 (3), 319 (1), 308 (3), 293 (4), 267 (3), 221 (2), 207 (10), 206 (15), 178(30), 165 (80). 89 (100).; Elemental analysis for C₂₁H₂₀N₂O₄ (Calcd./Found): C, 69.22/69.40; H, 5.53/5.56; N, 7.69/7.84.

3.2.1 General procedure for synthesis of 1,2,4,5-tetrasubstituted imidazoles. [ϵ -(2-(substituted phenyl)-4,5-diphenyl-1H-imidazol-1-yl)alkanoic acid] and [4-(2-(substituted phenyl)-4,5-diphenyl-1H-imidazol-1-yl)benzoic acid][25, 26].

In a rounded flask 50 mL add benzil (1.05 g, 5.0 mmol), an equivalent amount of the aldehyde (5 mmol), ammonium acetate (0.385g, 5 mmol), amino acid (5 mmol) and diethyl ammonium hydrogen sulfate catalyst (0.510 g, 3 mmol). The mixture was refluxed in an oil bath with stirring at 110 °C for about 35 min with following up the reaction with TLC using chloroform: ethanol (9:1) till reaction completes. The reaction mixture was poured on an iced water and the resulting precipitate was filtered off, washed with water and dried. The crude product was crystallized from ethanol.

3.2.2. Synthesis of diethyl ammonium hydrogen sulfate (DEAHS) [23].

Diethyl amine (22.2 g, 0.3 mol) was added into a 250 mL three-necked flask with a magnetic stirrer. Concentrated sulfuric acid (98%), 29.4 g (0.3 mol) was added dropwise to the flask at room temperature then heated to 80 °C for 12 h. The product was washed with diethyl ether three times to remove the traces of non-ionic material. The residue was dried under vacuum using a rotary evaporator to obtain the clear viscous product, diethyl ammonium hydrogen sulfate. Yield 98 %, pH 1.6.

4-(2-(4-Methoxyphenyl)-4,5-diphenyl-1H-imidazol-1-yl)benzoic acid (9a): white crystals; mp.328-330 °C (yield 92%) IR (cm⁻¹): 3214 (OH), 1687 (C=O), 1605 (C=N), 1068 (C-O); ¹H-NMR (400 MHz, DMSO-*d*₆) δ (ppm): 3.74 (s, 3H, O-CH₃), 6.86 (d, 2H, *J* = 8.80 Hz, 2 Ar-H), 6.88-7.50 (m, 10H, Ar-H), 7.51 (d, 2H, *J* = 8.80 Hz, 2 Ar-H), 7.82 (d, 2H, *J* = 8.80 Hz, 2 Ar-H), 7.84 (d, 2H, *J* = 8.80 Hz, 2 Ar-H); ¹³C-NMR (100 MHz, DMSO-*d*₆) δ (ppm): 55.65 (O-CH₃), 114.56, 124.17, 126.40, 126.57, 128.39, 129.22, 129.54, 130.58, 131.34, 131.76, 135.37, 136.58, 147.17, 160.122, 174.69 (OCO).; Elemental analysis for C₂₉H₂₂N₂O₃ (Calcd./Found): C, 78.01/78.27; H, 4.97/4.98; N, 6.27/6.42.

3-(2-(4-Methoxyphenyl)-4,5-diphenyl-1H-imidazol-1-yl)propanoic acid (9b): white crystals mp.200-202 °C (yield 87%); IR (cm⁻¹): 3398 (OH), 1717 (C=O), 1605 (C=N), 1040 (C-O); ¹H-

NMR (400 MHz, DMSO-*d*₆) δ (ppm); 2.87 (t, 2H, *J* = 6.80 Hz, **CH**₂-CO), 4.10 (t, 2H, *J* = 6.80 Hz, N-**CH**₂), 3.85 (s, 3H, O-**CH**₃), 7.08 (d, 2H, *J* = 8.80, 2 Ar-H), 7.68-7.10 (m, 10H, Ar-H), 8.00 (d, 2H, *J* = 8.80 Hz, 2 Ar-H); ¹³C-NMR (100 MHz, DMSO-*d*₆) δ (ppm): 32.51 (CH₂), 41.69 (NCH₂), 55.72 (O-CH₃), 114.54, 123.92, 126.52, 127.21, 128.44, 128.80, 129.34, 129.60, 129.74, 130.64, 131.35, 131.52, 135.24, 136.87, 147.09, 160.13, 171.95.; Elemental analysis for C₂₅H₂₂N₂O₃ (Calcd./Found): C, 75.36/75.64; H, 5.57/5.65; N, 7.03/7.19.

4-(2-(4-Methoxyphenyl)-4,5-diphenyl-1H-imidazol-1-yl)butanoic acid (9c): White crystals; mp.188-190 °C (yield 84%); IR (cm⁻¹): 3371 (OH), 1705 (C=O), 1607 (C=N), 1068 (C-O); ¹H-NMR (400 MHz, DMSO-*d*₆) δ (ppm): 1.53-1.54 (m, 2H, **CH**₂-CH₂-CO), 2.04 (t, 2H, *J* = 6.80 Hz, **CH**₂-CO), 3.85(t, 2H, *J* = 6.80 Hz, N-**CH**₂), 3.93 (s, 3H, O-**CH**₃), 7.09 (d, 2H, *J* = 8.80, 2 Ar-H), 7.18-7.53(m, 10H, Ar-H), 7.68 (d, 2H, *J* = 8.80 Hz, 2 Ar-H); ¹³C-NMR (100 MHz, DMSO-*d*₆) δ (ppm): 25.87 (CH₂), 31.40 (CH₂), 44.33 (NCH₂), 55.72 (O-CH₃), 114.56, 123.40, 126.43, 126.59, 128.39, 129.22, 129.54, 130.58, 131.34, 131.40, 134.62, 136.01, 145.09, 158.32, 174.08.; Elemental analysis for C₂₆H₂₄N₂O₃ (Calcd./Found): C, 75.71/75.94; H, 5.86/5.92; N, 6.79/6.84.

5-(2-(4-Methoxyphenyl)-4,5-diphenyl-1H-imidazol-1-yl)pentanoic acid (9d): White crystals; mp.156-158 °C (yield 71%); IR (cm⁻¹): 3373 (OH), 1703 (C=O), 1604 (C=N), 1076 (C-O); ¹H-NMR (400 MHz, DMSO-*d*₆) δ (ppm): 1.16-1.31 (m, 2H, CH₂-**CH**₂-CH₂-CO), 1.84 (m, 2H, **CH**₂-CH₂-CH₂-CO), 2.62 (t, 2H, *J* = 6.80 Hz, **CH**₂-CO), 3.85 (t, 2H, *J* = 6.80 Hz, N-**CH**₂), 3.85 (s, 3H, O-**CH**₃), 7.10 (d, 2H, *J* = 8.80, 2 Ar-H), 7.53-7.18 (m, 10H, Ar-H), 7.65 (d, 2H, *J* = 8.80 Hz, 2 Ar-H); ¹³C-NMR (100 MHz, DMSO-*d*₆) δ (ppm): 22.06 (CH₂), 29.81(CH₂), 33.97 (CH₂), 44.55 (NCH₂), 55.74(O-CH₃), 114.57, 123.40, 126.42, 126.59, 128.39, 129.22, 129.54, 130.58, 131.34, 131.40, 134.62, 136.01, 145.09, 158.32, 174.08.; Elemental analysis for C₂₇H₂₆N₂O₃ (Calcd./Found): C, 76.03/76.26; H, 6.14/6.20; N, 6.57/6.71.

6-(2-(4-Methoxyphenyl)-4,5-diphenyl-1H-imidazol-1-yl)hexanoic acid (9e): white crystals; mp.160-162 °C (yield 93%); IR (cm⁻¹): 3392 (OH), 1708 (C=O), 1606 (C=N), 1070 (C-O); ¹H-NMR (400 MHz, DMSO-*d*₆) δ (ppm): 1.17-1.30 (m, 2H, CH₂-**CH**₂-CH₂-CO), 1.30-1.52 (m, 4H, **CH**₂-**CH**₂-CH₂-CH₂-CO), 1.94 (t, 2H, *J* = 7.20 Hz, **CH**₂-CO), 3.84 (t, 2H, *J* = 7.20 Hz, N-**CH**₂), 3.84 (s, 3H, O-**CH**₃), 7.09 (d, 2H, *J* = 8.80, 2 Ar-H), 7.10-7.52 (m, 10H, Ar-H), 7.65 (d, 2H, *J* = 8.80 Hz, 2 Ar-H); ¹³C-NMR (100 MHz, DMSO-*d*₆) δ (ppm): 24.16 (CH₂), 25.71 (CH₂), 29.80 (CH₂), 34.03 (CH₂), 44.58 (NCH₂), 55.72 (O-CH₃), 114.56, 124.17, 126.40, 126.57, 128.39, 129.22, 129.54, 130.58, 131.34, 131.76, 135.37, 136.58, 147.17, 160.12, 174.69; EI-MS (70 eV)

m/z (%): 440 (70) (M⁺), 395 (1), 381 (3), 354 (9), 339 (14), 325 (29), 311 (12), 119 (66), 104 (100); Elemental analysis for C₂₈H₂₈N₂O₃ (Calcd./Found): C, 76.34/76.59; H, 6.41/6.48; N, 6.36/6.49.

4-(2-(4-Chlorophenyl)-4,5-diphenyl-1H-imidazol-1-yl)benzoic acid (10a): Yellowish white crystals; mp. 233-235 °C (yield 87%); IR ν (cm⁻¹): 3348 (OH), 1675 (C=O), 1625 (C=N), 1076 (C-O); ¹H-NMR (400 MHz, DMSO-*d*₆) δ (ppm): 6.58 (d, 2H, *J* = 8.80, 2 Ar-H), 7.59-7.31(m, 10H, Ar-H), 7.61 (d, 2H, *J* = 8.80 Hz, 2 Ar-H), 7.68 (d, 2H, *J* = 8.80 Hz, 2 Ar-H), 7.98 (d, 2H, *J* = 8.80 Hz, 2 Ar-H); ¹³C-NMR (100 MHz, DMSO-*d*₆) δ (ppm): 113.13, 118.56, 121.24, 129.46, 129.80, 130.94, 131.59, 134.00, 134.76, 135.37, 139.58, 151.17, 154.19, 161.17, 169.42; Elemental analysis for C₂₈H₁₉ClN₂O₂ (Calcd./Found): C, 74.58/74.80; H, 4.25/4.23; N, 6.21/6.34.

3-(2-(4-Chlorophenyl)-4,5-diphenyl-1H-imidazol-1-yl)propanoic acid (10b): Brownish white crystals mp. 226-228 °C (yield 89%); IR ν (cm⁻¹): 3375-2766 (OH), 1709 (C=O), 1601 (C=N), 1081 (C-O); ¹H-NMR (400 MHz, DMSO-*d*₆) δ (ppm): 2.29 (t, 2H, *J* = 6.80 Hz, CH₂-CO), 4.15 (t, 2H, *J* = 6.80 Hz, N-CH₂), 7.13 (d, 2H, *J* = 8.80, 2 Ar-H), 7.15-7.63 (m, 10H, Ar-H), 7.80 (d, 2H, *J* = 8.80 Hz, 2 Ar-H); ¹³C-NMR (100 MHz, DMSO-*d*₆) δ (ppm): 32.57 (CH₂), 41.75 (NCH₂), 126.60, 126.66, 127.7, 127.85, 128.46, 129.14, 129.48, 129.63, 130.43, 130.99, 131.33, 132.74, 135.00, 137.29, 148.42, 174.08 (OCO); Elemental analysis for C₂₄H₁₉ClN₂O₂ (Calcd./Found): C, 71.55/71.82; H, 4.75/4.79; N, 6.95/7.13.

4-(2-(4-Chlorophenyl)-4,5-diphenyl-1H-imidazol-1-yl)butanoic acid (10c): Brown crystals; mp. 193-195 °C (yield 85%); IR ν (cm⁻¹): 3371 (OH), 1698 (C=O), 1604 (C=N), 1082 (C-O); ¹H-NMR (400 MHz, DMSO-*d*₆) δ (ppm): 1.74-1.83 (m, 2H, CH₂-CH₂-CO), 2.84 (t, 2H, *J* = 6.80 Hz, CH₂-CO), 3.94 (t, 2H, *J* = 6.80 Hz, N-CH₂), 7.13 (d, 2H, *J* = 8.80, 2 Ar-H), 7.14-7.59 (m, 10H, Ar-H), 7.81 (d, 2H, *J* = 8.80 Hz, 2 Ar-H); ¹³C-NMR (100 MHz, DMSO-*d*₆) δ (ppm): 25.96 (CH₂), 31.51 (CH₂), 44.51 (NCH₂), 126.63, 126.66, 127.70, 127.85, 128.44, 129.14, 129.37, 129.58, 130.43, 130.88, 131.32, 132.74, 135.00, 137.29, 148.42, 174.08 (OCO). EI-MS (70 eV) m/z (%): 418 (39) (M⁺), 416 (100) (M⁺), 371 (1), 357 (3), 343 (7), 330 (36), 178 (19). Elemental analysis for C₂₅H₂₁ClN₂O₂ (Calcd./Found): C, 72.02/72.23; H, 5.08/5.17; N, 6.72/6.89.

5-(2-(4-Chlorophenyl)-4,5-diphenyl-1H-imidazol-1-yl)pentanoic acid (10d): White crystals; mp. 158-160 °C; (yield 70%); IR (cm⁻¹): 3374 (OH), 1700 (C=O), 1600 (C=N), 1072 (C-O); ¹H-NMR (400 MHz, DMSO-*d*₆) δ (ppm): 1.32-1.33 (m, 2H, CH₂-CH₂-CH₂-CO), 1.87-1.89 (m, 2H, CH₂-CH₂-CH₂-CO), 2.83 (t, 2H, *J* = 6.80 Hz, CH₂-CO), 3.91 (t, 2H, *J* = 6.80 Hz, N-CH₂), 7.12

(d, 2H, $J = 8.80$ Hz, 2 Ar-H), 6.14-7.60 (m, 10H, Ar-H), 7.76-7.78 (d, 2H, $J = 8.80$ Hz, 2 Ar-H); ^{13}C -NMR (100 MHz, DMSO- d_6) δ (ppm): 21.93 (CH_2), 29.75(CH_2), 41.79 (CH_2), 44.67 (NCH_2), 126.61, 126.66, 127.7, 127.85, 128.44, 129.17, 129.38, 129.57, 130.65, 130.84, 131.34, 132.74, 135.00, 137.96, 148.42, 178.55.; Elemental analysis for $\text{C}_{26}\text{H}_{23}\text{ClN}_2\text{O}_2$ (Calcd./Found): C, 72.47/72.65; H, 5.38/5.44; N, 6.50/6.67.

6-(2-(4-Chlorophenyl)-4,5-diphenyl-1H-imidazol-1-yl)hexanoic acid(10e): White crystals; mp.166-168 °C: (yield 93%); IR (cm^{-1}): 3400 (OH), 1703 (C=O), 1600 (C=N), 1087 (C-O); ^1H -NMR (400 MHz, DMSO- d_6) δ (ppm): 1.19-1.32 (m, 4H, $\text{CH}_2\text{-CH}_2\text{-CH}_2\text{-CO}$), 1.52-1.60 (m, 2H, $\text{CH}_2\text{-CH}_2\text{-CH}_2\text{-CH}_2\text{-CO}$), 1.94 (t, 2H, $J = 7.20$ Hz, $\text{CH}_2\text{-CO}$), 3.88 (t, 2H, $J = 7.20$ Hz, N- CH_2), 7.12 (d, 2H, $J = 8.80$, 2 Ar-H), 7.17-7.60 (m, 10H, Ar-H), 7.75-7.77 (d, 2H, $J = 8.80$ Hz, 2 Ar-H); ^{13}C -NMR (100 MHz, DMSO- d_6) δ (ppm): 24.66 (CH_2), 26.55 (CH_2), 29.79 (CH_2), 34.67 (CH_2), 44.71 (NCH_2), 126.57, 127.7, 128.47, 128.85, 129.19, 129.40, 129.59, 130.58, 130.87, 131.32, 134.00, 135.04, 137.06, 137.24, 145.96, 174.82.; Elemental analysis for $\text{C}_{27}\text{H}_{25}\text{ClN}_2\text{O}_2$ (Calcd./Found): C, 72.88/73.21; H, 5.66/5.73; N, 6.30/6.46.

4-(2,4,5-Triphenyl-1H-imidazol-1-yl)benzoic acid (11a): White crystals; mp.286-290 °C; (yield 91%); IR (cm^{-1}): 3357 (OH), 1690 (C=O), 1601 (C=N), 1066 (C-O); ^1H -NMR (400 MHz, DMSO- d_6) δ (ppm): 7.26 (d, 2H, $J = 8.80$, 2 Ar-H), 7.31-7.41 (m, 13H, Ar-H), 7.54 (d, 2H, $J = 8.80$ Hz, 2 Ar-H), 7.84 (d, 2H, $J = 8.80$ Hz, 2 Ar-H); ^{13}C -NMR (100 MHz, DMSO- d_6) δ (ppm): 113.13, 126.90, 126.96, 128.57, 128.65, 128.82, 128.86, 129.06, 130.35, 131.60, 132.12, 134.37, 136.58, 139.12, 147.17, 168.69; EI-MS (70 eV) m/z (%): 416 (5) (M^+), 347 (4), 339 (8), 325 (18), 311 (7) 281 (5), 264 (4), 222 (8), 140 (19), 89 (53), 69 (100).; Elemental analysis for $\text{C}_{28}\text{H}_{20}\text{N}_2\text{O}_2$ (Calcd./Found): C, 80.75/81.02; H, 4.84/4.87; N, 6.73/6.95.

3-(2,4,5-Triphenyl-1H-imidazol-1-yl)propanoic acid (11b): White crystals; mp.149-152°C (yield 84%); IR v (cm^{-1}): 3380 (OH), 1711 (C=O), 1601(C=N), 1071 (C-O); ^1H -NMR (400 MHz, DMSO- d_6) δ (ppm); 2.22 (t, 2H, $J = 6.80$ Hz, $\text{CH}_2\text{-CO}$), 4.12 (t, 2H, $J = 6.80$ Hz, N- CH_2), 7.13-7.54 (m, 13H, Ar-H), 7.74 (d, $J = 7.8$ Hz, 2H, 2 Ar-H).; ^{13}C -NMR (100 MHz, DMSO- d_6) δ (ppm): 35.78 (CH_2), 41.67 (NCH_2), 125.73, 126.54, 126.58, 128.43, 128.63, 128.80, 129.04, 129.23, 129.38, 129.59, 130.43, 131.36, 135.40, 137.29, 148.42, 173.55 (OCO). EI-MS (70 eV) m/z (%): 368 (66) (M^+), 323 (9), 309 (3), 296 (100), 165 (68); Elemental analysis for $\text{C}_{24}\text{H}_{20}\text{N}_2\text{O}_2$ (Calcd./Found): C, 78.24/78.41; H, 5.47/5.54; N, 7.60/7.76.

4-(2,4,5-Triphenyl-1H-imidazol-1-yl)butanoic acid (11c): White crystals; mp.179-181°C; (yield 87%); IR (cm⁻¹): 3370 (OH), 1709 (C=O), 1604 (C=N), 1069 (C-O); ¹H-NMR (400 MHz, DMSO-*d*₆) δ (ppm): 1.82-1.89 (m, 2H, CH₂-CH₂-CO), 2.85 (t, 2H, *J* = 6.80 Hz, CH₂-CO), 3.96 (t, 2H, *J* = 6.80 Hz, N-CH₂), 7.13 (d, *J* = 7.8 Hz, 2H, 2 Ar-H), 7.19-7.75 (m, 13H, Ar-H); ¹³C-NMR (100 MHz, DMSO-*d*₆) δ (ppm): 26.07 (CH₂), 31.73 (CH₂), 44.47 (NCH₂), 125.73, 126.53, 126.62, 128.43, 128.63, 128.42, 129.05, 129.16, 129.30, 129.56, 130.43, 131.34, 135.40, 137.29, 148.42, 173.60; Elemental analysis for C₂₅H₂₂N₂O₂ (Calcd./Found): C, 78.51/78.67; H, 5.80/5.86; N, 7.32/7.49.

5-(2,4,5-Triphenyl-1H-imidazol-1-yl)pentanoic acid (11d): White crystals; mp.130-132°C (yield 78%); IR (cm⁻¹): 3380 (OH), 1732 (C=O), 1601 (C=N), 1072 (C-O); ¹H-NMR (400 MHz, DMSO-*d*₆) δ (ppm): 1.32-1.36 (m, 2H, CH₂-CH₂-CH₂-CO), 1.86 (m, 2H, CH₂-CH₂-CH₂-CO), 2.83 (t, 2H, *J* = 6.80 Hz, CH₂-CO), 3.91 (t, 2H, *J* = 6.80 Hz, N-CH₂), 7.13 (d, *J* = 7.8 Hz, 2H, 2 Ar-H), 7.19-7.73 (m, 13H, Ar-H); ¹³C-NMR (100 MHz, DMSO-*d*₆) δ (ppm): 21.88 (CH₂), 29.75 (CH₂), 33.57 (CH₂), 44.57 (NCH₂), 126.52, 126.59, 128.42, 128.63, 128.80, 129.06, 129.16, 129.19, 129.30, 129.55, 131.35, 131.55, 135.40, 137.29, 148.42, 173.55; Elemental analysis for C₂₆H₂₄N₂O₂ (Calcd./Found): C, 78.76/78.98; H, 6.10/6.19; N, 7.07/7.30.

6-(2,4,5-Triphenyl-1H-imidazol-1-yl)hexanoic acid (11e): White crystals; mp.146-148°C (yield 94%); IR (cm⁻¹): 3393 (OH), 1698 (C=O), 1601 (C=N), 1069 (C-O); ¹H-NMR (400 MHz, DMSO-*d*₆) δ (ppm): 1.19-1.29 (m, 2H, CH₂-CH₂-CH₂-CO), 1.52-1.78 (m, 4H, CH₂-CH₂-CH₂-CH₂-CO), 1.94 (t, 2H, *J* = 7.20 Hz, CH₂-CO), 3.88 (t, 2H, *J* = 7.20 Hz, N-CH₂), 7.12 (d, *J* = 7.8 Hz, 2H, 2 Ar-H), 7.19-7.72 (m, 13H, Ar-H); ¹³C-NMR (100 MHz, DMSO-*d*₆) δ (ppm): 24.14 (CH₂), 25.70 (CH₂), 29.80 (CH₂), 34.05 (CH₂), 44.64 (NCH₂), 126.50, 126.58, 128.41, 128.63, 128.80, 129.05, 129.19, 129.29, 129.55, 131.34, 131.55, 135.40, 137.29, 148.42, 173.55; Elemental analysis for C₂₇H₂₆N₂O₂ (Calcd./Found): C, 79.00/79.23; H, 6.38/6.46; N, 6.82/6.98.

4. Biological evaluation

4.1. Anticonvulsant activity screening

Evaluating the preliminary anticonvulsant activities and neurotoxicity of all newly synthesized compounds with respect to that of valproate sodium and diphenylhydantoin sodium as reference drugs. The biological evaluation was done according to the protocol given by the epilepsy section of National Institute of Neurological Disorders and Stroke (NINDS) using the standard protocol adopted by the Antiepileptic Drug Development (ADD) program [27] which includes the maximal

electroshock seizure (MES) screen, the subcutaneous pentylenetetrazole (s.c.PTZ) screen, and the rotarod (neurotoxicity) test. In addition, the selected highest potent compounds were subjected to the quantitative estimation (median effective dose, ED₅₀).

4.1.1. Materials and methods

In this study, adult male Swiss albino mice, weighing 19-25g, were used. Animals were purchased from Animal House Colony of the National Research Centre, Cairo, Egypt. The mice were housed under standardized conditions (room temperature $23 \pm 2^\circ\text{C}$; relative humidity $55 \pm 5\%$; 12 h light / dark cycle) and allowed free access to tap water and standard mice chow throughout the whole experimental period. All animal procedures were performed in conformity with the recommendations for the proper care and use of laboratory animals following the regulations of the ethical committee of the National Research Centre, Cairo, Egypt. The animals were randomly assigned to test, reference and control experimental groups consisting of 6-8 mice each after 7 days of their adaptation to laboratory conditions.

Tween-80 (7%) was used as a vehicle in which all the test compounds were suspended. The two primary anticonvulsant screens MES and s.c. PTZ were performed in mice at the dose 100 mg/kg. Further investigations were done on the most active compounds in mice i.p. at different doses for the quantification of their anticonvulsant activity and neurotoxicity.

4.1.2. Chemicals and drugs

Tween-80, pentylenetetrazol and valproate sodium were purchased from Sigma (Sigma, St. Lewis, USA), diphenylhydantoin sodium obtained from (DPHS, Nasr Co., Egypt).

4.2. Methods

4.2.1. Maximal electroshock seizure (MES) test

The maximal electroshock seizure (MES) screen is indicative of the ability of the test compounds to prevent seizure attack and their ability to protect against generalized tonic-clonic seizure [27]. In this test, after half an hour of intraperitoneal injection of the tested compounds by a current (fixed current intensity of 25 mA, 0.2s stimulus duration) delivered *via* ear clip electrodes by a Roden Shocker Generator (constant-current stimulator Type 221, Hugo Sachs Elektronik, Freiburg, Germany) [19, 36], the electro convulsions were produced.

The principle for the occurrence of seizure activity was the tonic hind limb extension (i.e. the hind limbs of animals outstretched 180° to the plane of the body axis). The anticonvulsant potential of

the compounds under investigation was compared with that of diphenylhydantoin sodium as a reference drug.

4.2.2. Subcutaneous pentylenetetrazol (s.c. PTZ) test

PTZ- induced clonic seizures are widely used as a model that predicts drugs effectiveness in decreasing the seizure threshold and active against generalized seizures of the petit mal (absence) type [37, 38].

Aqueous solution of PTZ at a dose level of 85 mg/kg [39] was injected subcutaneously under a loose fold of skin on the back of the mouse's neck. Tonic-extensor convulsions in at least 97% of controls were induced by this dose. The test compounds were injected intraperitoneally to the mice 30 minutes before PTZ administration. In single cages, the mice were placed and observed for 30 minutes for the loss of righting reflexes lasting for at least 3 second. After PTZ treatment [40, 41], as the absence of loss of righting reflexes was chosen as an index for protective effect. The dose of compounds and reference standard that induced maximum percentage protection was evaluated. The studied biological activity of the tested compounds was compared with the reference standard, valproate sodium. The ED₅₀ of the most potent compounds were calculated according to the method of Litchfield and Wilcoxon [20, 42].

4.3. Rotarod (neurotoxicity) test

Neurological toxicity (NT) in mice was determined by rotarod test mentioned in the method reported by Dunham and Miya. In brief, a group of animals (groups of 6 mice) were trained to balance on a rotating rod (3 cm diameter and 6 rpm speed) and they were allowed three attempts to remain on the rotating rod for 1 minute. The trained animals were treated with the tested compounds at dose level by intraperitoneal injection.

The test compounds were neurotoxic at a particular dose level if the trained animal showed lack of Rolling Roller Performance [i.e the animals showing neurological deficits (ataxia and sedation), as indicated by the inability to keep equilibrium on the rod for at least 1 minute in each of three trials]. The trained animals were tested, in this manner, after 30 minute of the drug administration, and the neurotoxic effect was recorded and compared with those animals given phenytoin [43].

5. Virtual screening using shape similarity by ROCS

The principal of representing shape and color features in ROCS is using ROCS application OpenEye scientific software [29]. Phenytoin, and valporic acid were chosen as query molecules. A library of final compounds was adopted as the database file. Omega application in OpenEye

scientific software was used for energy minimizing of both query and database files. vROCS was employed to run and analyze/visualize the results. Compounds conformers were scored based upon the Gaussian overlap to the query and the best scoring parameters is Tanimoto Combo scores (shape + color) the highest score is the best matched with query compound. The quality of alignment between database and query was calculated using Tanimoto Combo. Tanimoto Combo is the summation of Shape Tanimoto and Color Tanimoto. Shape Tanimoto represents the shared volume and mismatch volume and has scale from 0 to 1. Color Tanimoto (scale from 0 to 1) is reflective of the degree of matching or mismatching of light chemical features in 3 dimensions. Using fragment disconnected non-chemically meaning pieces of a molecule, both query and database molecules are combined into a single species.

6. References:

- [1] I. Megiddo, A. Colson, D. Chisholm, T. Dua, A. Nandi, R. Laxminarayan, Health and economic benefits of public financing of epilepsy treatment in India: An agent-based simulation model, *Epilepsia* 57(3) (2016) 464-474.
- [2] R. Kumar, T. Singh, H. Singh, S. Jain, R. Roy, Design, synthesis and anticonvulsant activity of some new 6, 8-halo-substituted-2h-[1, 2, 4] triazino [5, 6-b] indole-3 (5h)-one/-thione and 6, 8-halo-substituted 5-methyl-2h-[1, 2, 4] triazino [5, 6-b] indol-3 (5h)-one/-thione, *EXCLI journal* 13 (2014) 225.
- [3] D.H. Tang, D.C. Malone, T.L. Warholak, J. Chong, E.P. Armstrong, M.K. Slack, C.-H. Hsu, D.M. Labiner, Prevalence and incidence of epilepsy in an elderly and low-income population in the United States, *Journal of Clinical Neurology* 11(3) (2015) 252-261.
- [4] H.M. Neels, A.C. Sierens, K. Naelaerts, S.L. Scharpe, G.M. Hatfield, W.E. Lambert, Therapeutic drug monitoring of old and newer anti-epileptic drugs, *Clinical Chemistry and Laboratory Medicine (CCLM)* 42(11) (2004) 1228-1255.
- [5] M. Bialer, S.I. Johannessen, R.H. Levy, E. Perucca, T. Tomson, H.S. White, Progress report on new antiepileptic drugs: a summary of the Tenth Eilat Conference (EILAT X), *Epilepsy research* 92(2) (2010) 89-124.
- [6] H.H. Refsgaard, B.F. Jensen, P.B. Brockhoff, S.B. Padkjær, M. Guldbandt, M.S. Christensen, In silico prediction of membrane permeability from calculated molecular parameters, *Journal of medicinal chemistry* 48(3) (2005) 805-811.
- [7] P.P. Bose, U. Chatterjee, I. Hubatsch, P. Artursson, T. Govender, H.G. Kruger, M. Bergh, J. Johansson, P.I. Arvidsson, In vitro ADMET and physicochemical investigations of poly-N-methylated peptides designed to inhibit A β aggregation, *Bioorganic & medicinal chemistry* 18(16) (2010) 5896-5902.

- [8] T. Hou, J. Wang, W. Zhang, X. Xu, ADME evaluation in drug discovery. 7. Prediction of oral absorption by correlation and classification, *Journal of chemical information and modeling* 47(1) (2007) 208-218.
- [9] C.A. Lipinski, F. Lombardo, B.W. Dominy, P.J. Feeney, Experimental and computational approaches to estimate solubility and permeability in drug discovery and development settings, *Advanced drug delivery reviews* 23(1-3) (1997) 3-25.
- [10] C.A. Lipinski, F. Lombardo, B.W. Dominy, P.J. Feeney, Experimental and computational approaches to estimate solubility and permeability in drug discovery and development, *Advanced Drug Delivery Reviews* 46 (2001) 3-26.
- [11] R. Wang, Y. Fu, L. Lai, A new atom-additive method for calculating partition coefficients, *Journal of chemical information and computer sciences* 37(3) (1997) 615-621.
- [12] J. Dimmock, S. Vashishtha, J. Stables, Ureylene anticonvulsants and related compounds, *Die Pharmazie* 55(7) (2000) 490-494.
- [13] J.R. Dimmock, S.C. Vashishtha, J.P. Stables, Anticonvulsant properties of various acetylhydrazones, oxamoylhydrazones and semicarbazones derived from aromatic and unsaturated carbonyl compounds, *European journal of medicinal chemistry* 35(2) (2000) 241-248.
- [14] G.H. Glaser, J.K. Penry, D.M. Woodbury, *Antiepileptic drugs: Mechanisms of action*, Raven Press 1980.
- [15] M. Wong, J. Defina, P. Andrews, Conformational analysis of clinically active anticonvulsant drugs, *Journal of medicinal chemistry* 29(4) (1986) 562-572.
- [16] N. Shalmali, M.R. Ali, S. Bawa, Imidazole: an essential edifice for the identification of new lead compounds and drug development, *Mini reviews in medicinal chemistry* 18(2) (2018) 142-163.
- [17] R. Vroemans, F. Bamba, J. Winters, J. Thomas, J. Jacobs, L. Van Meervelt, J. John, W. Dehaen, Sequential Ugi reaction/base-induced ring closing/IAAC protocol toward triazolobenzodiazepine-fused diketopiperazines and hydantoins, *Beilstein journal of organic chemistry* 14(1) (2018) 626-633.
- [18] C.S. Kumar, B. Veeresh, K.C. Ramesha, C.S. Raj, K.M. Mahadevaiah, S.B. Prasad, Synthesis and Evaluation of Novel Diazaspiro Hydantoins as Potential Anticonvulsants, *Central Nervous System Agents in Medicinal Chemistry (Formerly Current Medicinal Chemistry-Central Nervous System Agents)* 17(3) (2017) 201-208.
- [19] K. Metwally, O. Aly, S. El-Nabtity, Spirohydantoins derived from 1-tetralone: design, synthesis and exploration of their anticonvulsant activity and neurotoxicity, *Bull Fac Pharm Cairo Univ* 45 (2007) 149-154.
- [20] A.H. Abuelhassan, M.M. Badran, H.A. Hassan, D. Abdelhamed, S. Elnabtity, O.M. Aly, Design, synthesis, anticonvulsant activity, and pharmacophore study of new 1, 5-diaryl-1H-1, 2, 4-triazole-3-carboxamide derivatives, *Medicinal Chemistry Research* 27(3) (2018) 928-938.
- [21] J.J. Li, *Bucherer—Bergs reaction*, *Name Reactions*, Springer 2009, pp. 76-77.

- [22] H. Nagasawa, J. Elberling, F. Shirota, 2-Aminoadamantane-2-carboxylic acid, a rigid, achiral, tricyclic. alpha.-amino acid with transport inhibitory properties, *Journal of medicinal chemistry* 16(7) (1973) 823-826.
- [23] S.K. Mohamed, J. Simpson, A.A. Marzouk, A.H. Talybov, A.A. Abdelhamid, Y.A. Abdullayev, V.M. Abbasov, Multicomponent green synthesis, spectroscopic and structural investigation of multi-substituted imidazoles. Part 1, *Zeitschrift für Naturforschung B* 70(11) (2015) 809-817.
- [24] A.A. Marzouk, A.M. Abu-Dief, A.A. Abdelhamid, Hydrothermal preparation and characterization of ZnFe₂O₄ magnetic nanoparticles as an efficient heterogeneous catalyst for the synthesis of multi-substituted imidazoles and study of their anti-inflammatory activity, *Applied Organometallic Chemistry* 32(1) (2018) e3794.
- [25] A.M. Abu-Dief, L.H. Abdel-Rahman, A.A. Abdelhamid, A.A. Marzouk, M.R. Shehata, M.A. Bakheet, O.A. Almaghrabi, A. Nafady, Synthesis and characterization of new Cr (III), Fe (III) and Cu (II) complexes incorporating multi-substituted aryl imidazole ligand: Structural, DFT, DNA binding, and biological implications, *Spectrochimica Acta Part A: Molecular and Biomolecular Spectroscopy* 228 (2020) 117700.
- [26] A.A. Abdelhamid, H.A. Salah, A.A. Marzouk, Synthesis of imidazole derivatives: Ester and hydrazide compounds with antioxidant activity using ionic liquid as an efficient catalyst, *Journal of Heterocyclic Chemistry* (2019) 1-10.
- [27] R.J. Porter, J. Cereghino, G.D. Gladding, B. Hessie, H.J. Kupferberg, B. Scoville, B.G. White, Antiepileptic drug development program, *Cleveland Clinic Quarterly* 51(2) (1984) 293-305.
- [28] N. Dunham, T. Miya, A note on a simple apparatus for detecting neurological deficit in rats and mice, *Journal of the American Pharmaceutical Association* 46(3) (1957) 208-209.
- [29] ROCS, Shape Similarity for Virtual Screening & Lead Hopping; .
- [30] P.C. Hawkins, A.G. Skillman, A. Nicholls, Comparison of shape-matching and docking as virtual screening tools, *Journal of medicinal chemistry* 50(1) (2007) 74-82.
- [31] J.J. Sutherland, R.K. Nandigam, J.A. Erickson, M. Vieth, Lessons in molecular recognition. 2. Assessing and improving cross-docking accuracy, *Journal of chemical information and modeling* 47(6) (2007) 2293-2302.
- [32] K.R. Abdellatif, W.A. Fadaly, Y.A. Elshaier, W.A. Ali, G.M. Kamel, Non-acidic 1, 3, 4-trisubstituted-pyrazole derivatives as lonazolac analogs with promising COX-2 selectivity, anti-inflammatory activity and gastric safety profile, *Bioorganic chemistry* 77 (2018) 568-578.
- [33] [Molinspiration Cheminformatics. www.molinspiration.com].
- [34] [<http://molsoft.com/mprop>].
- [35] [tps://preadmet.bmdrc.kr/toxicity].
- [36] N.O. Mahmoodi, Z. Khodaei, Evaluating the one-pot synthesis of hydantoins, *Arkivoc* 3 (2007) 29-36.
- [37] W. Löscher, New visions in the pharmacology of anticonvulsion, *European Journal of Pharmacology* 342(1) (1998) 1-13.

- [38] J.M. Rho, R. Sankar, The pharmacologic basis of antiepileptic drug action, *Epilepsia* 40(11) (1999) 1471-1483.
- [39] D. Woodbury, Applications to drug evaluations, *Experimental Models of Epilepsy* (1972) 557-583.
- [40] R. Fariello, R. McArthur, A. Bonsignori, M. Cervini, R. Maj, P. Marrari, P. Pevarello, H. Wolf, J. Woodhead, H.S. White, Preclinical evaluation of PNU-151774E as a novel anticonvulsant, *Journal of Pharmacology and Experimental Therapeutics* 285(2) (1998) 397-403.
- [41] W. Löscher, D. Hönack, C.P. Fassbender, B. Nolting, The role of technical, biological and pharmacological factors in the laboratory evaluation of anticonvulsant drugs. III. Pentylenetetrazole seizure models, *Epilepsy research* 8(3) (1991) 171-189.
- [42] M.H. Estrada, H. Insuasty, L.E. Cuca, M. Marder, A. Fierro, M.F. Guerrero, Anticonvulsant profile of 2-ethylthio-7-methyl-4-(4-methylphenyl) pyrazolo [1, 5-a][1, 3, 5] triazine, *Brazilian Journal of Pharmaceutical Sciences* 50(1) (2014) 73-81.
- [43] J.a. LITCHFIELD, F. Wilcoxon, A simplified method of evaluating dose-effect experiments, *Journal of pharmacology and experimental therapeutics* 96(2) (1949) 99-113.

Table 1: The anticonvulsant activity and percentage mortality prevention of the target compounds against MES induced seizures in mice in comparison with phenytoin.

Compound	Dose		Electric shock protection (%)	Mortality prevention (%)
	mg/kg	mmol/kg		
2	100	0.400	50	100
3a	100	0.295	16.66	66.66
3b	100	0.285	33.33	33.33
3c	100	0.274	0.00	100
3d	100	0.255	33.33	100
3e	100	0.251	0.00	100
4a	100	0.324	0.00	100
4b	100	0.310	0.00	33.33
4c	100	0.297	16.66	33.33
4d	100	0.274	0.00	100
4e	100	0.260	33.33	66.66
9a	100	0.224	0.00	100
9b	100	0.250	0.00	50
9c	100	0.242	0.00	50
9d	100	0.234	0.00	66.66
9e	100	0.227	0.00	66.66
10a	100	0.222	0.00	100
10b	100	0.248	0.00	100
10c	100	0.240	0.00	100
10d	100	0.232	0.00	100
10e	100	0.225	0.00	100
11a	100	0.240	0.00	100

11b	100	0.271	0.00	33.33
11c	100	0.261	0.00	33.33
11d	100	0.252	0.00	33.33
11e	100	0.243	0.00	66.66
Control	0	0	0	0
Phenytoin	100	0.396	100	100

Table 2: Anticonvulsant activity of the target compounds against s.c. PTZ-induced seizures in comparison with valproate sodium.

Compound	Dose		PTZ- Protection (%)	Relative potency to standard
	mg/kg	mmol/kg		
2	100	0.400	83.33	100
3a	100	0.295	33.33	39.99
3b	100	0.285	83.33	100
3c	100	0.274	50.00	60.00
3d	100	0.255	100.00	120.00
3e	100	0.251	66.66	80.00
4a	100	0.324	16.67	20.00
4b	100	0.310	50.00	60.00
4c	100	0.297	83.33	100
4d	100	0.274	50.00	60.00
4e	100	0.260	100.00	120.00
9a	100	0.224	66.66	80.00
9b	100	0.250	50	60.00
9c	100	0.242	50	60.00
9d	100	0.234	83.33	100
9e	100	0.227	50	60.00
10a	100	0.222	66.66	80.00
10b	100	0.248	66.66	80.00
10c	100	0.240	50	60.00
10d	100	0.232	33.33	39.99
10e	100	0.225	83.33	100
11a	100	0.240	83.33	100
11b	100	0.271	100	120.00
11c	100	0.261	66.66	80.00
11d	100	0.252	16.66	20.00
11e	100	0.243	100	120.00
Control	0	0	0	0
Valproate sodium	100	0.602	83.33	100

Table 3: The median effective dose (ED₅₀) for compounds **3d**, **4e** and **11b** against s.c. PTZ induced seizures.

Compound	Dose (mg/kg)	PTZ-Protection	PTZ-Protection (%)	Mortality prevention (%)	Onset of convulsion per unprotected animal	ED ₅₀	
3d	100	(6/6)	100	100			
	80	(5/6)	83.33	83.33	after 6 min.	55	
	60	(3/6)	50	83.33	after 4, 8 & 23 min.		
	40	(2/6)	33.33	66.66	after 6, 10, 15 & 25 min.		
4e	100	(6/6)	100	100			
4e	80	(5/6)	83.33	100	after 10 min.	60	
	60	(4/6)	66.66	83.33	after 6 & 8 min.		
11b	40	(1/6)	16.67	83.33	after 8, 10, 12, 18 & 2 min.		
	100	(6/6)	100	100			
	80	(4/6)	66.66	100	after 10 & 14 min.	50	
	60	(4/6)	66.66	83.33	after 10 & 23 min.		
	40	(3/6)	50	50	after 5, 11 & 15 min.		
	20	(2/6)	33.33	50	after 8, 12, 15 & 15 min.		

Table 4: Neurotoxicity (Rotarod test) screening data of (**3a-e**), (**4a-e**), (**9a-e**), (**10a-e**) and (**11a-e**) in mice with comparison to that of phenytoin.

Cmpd	Neurotoxicity	Neurotoxicity%	Cmpd	Neurotoxicity	Neurotoxicity%
2	(4/6)	66.66	9d	(3/6)	50
3a	(6/6)	100	9e	(6/6)	100
3b	(6/6)	100	10a	(0/6)	0
3c	(6/6)	100	10b	(0/6)	0
3d	(5/6)	83.33	10c	(0/6)	0
3e	(5/6)	83.33	10d	(0/6)	0
4a	(0/6)	0	10e	(0/6)	0
4b	(0/6)	0	11a	(0/6)	0
4c	(0/6)	0	11b	(0/6)	0
4d	(0/6)	0	11c	(0/6)	0
4e	(0/6)	0	11d	(0/6)	0
9a	(0/6)	0	11e	(0/6)	0
9b	(0/6)	0	Control	(0/6)	0
9c	(0/6)	0	Phenytoin	(3/6)	50

Table 5: Cytotoxicity studies for compounds (3d, 4e and 11b).

Compound	ED ₅₀ (S-PTZ, mg/kg)	LD ₅₀ (mg/kg)	PI
3d	55	630	11.45
4e	60	622	10.3
11b	50	610	12.2

ED₅₀= median effective dose in 50% of animals

LD₅₀= median toxic dose eliciting minimal neurological toxicity in 50% of animals

PI= protective index (TD₅₀/ED₅₀)

Table 6: Tanimoto Combo scores for all compounds in comparison to phenytoin and valporic acid.

		Tanimoto Combo Scores, Phenytoin as query	Tanimoto Combo Scores, Valporic acid as query
	Phenytoin	2	0.704
	Valporic	0.73	2
1	3a	1.2	0.53
2	10c	0.71	0.53
3	4c	1.14	0.52
4	4a	1.2	0.52
5	4b	1.16	0.54
6	10e	0.717	0.52
7	11b	0.713	0.52
8	3b	1.2	0.51
9	10b	0.70	0.51
10	3d	1.12	0.51
11	4d	1.07	0.50
12	11c	0.69	0.50
13	3c	1.20	0.50
14	11e	0.72	0.50
15	9e	0.69	0.49
16	9c	0.68	0.49
17	9b	0.69	0.48
18	10d	0.76	0.47
19	9d	0.72	0.45
20	4e	1.01	0.44
21	11d	0.75	0.44
22	3e	1.08	0.42
23	11a	0.716	0.37
24	10a	0.70	0.36

25	9a	0.68	0.35
----	----	------	------

Table 7: Predicted of pharmacokinetic and pharmacodynamic parameters compounds and standard drugs

Compound	Lipniski rule of five					TPSA	No. violations	Drug-likeness model score	BBB	PPB	HIA	
	Mwt	NRB	HBA	HBD	LogP							
1	Phentyoin	252.27	2	2	2	2.18	58.20	0	0.12	0.92	96.58	92.53
	Valporic	144.21	5	2	1	2.80	37.30	0	0.20	0.91	100.00	93.71
2	3a	336.35	4	5	1	2.15	75.71	0	-1.43	0.05	86.30	96.44
3	10c	416.91	7	3	1	5.72	55.12	1	0.79	0.44	100.00	97.62
4	4c	336.35	4	4	2	2.15	86.71	0	-0.83	0.26	54.62	96.27
4	4a	308.29	2	4	2	0.69	86.71	0	-1.02	0.36	90.58	95.32
5	4b	322.32	3	4	2	1.88	86.71	0	-0.95	0.36	92.58	95.85
6	10e	444.96	9	3	1	6.93	55.12	1	0.83	0.21	100.00	97.73
7	11b	368.44	6	3	1	4.97	55.12	1	-0.12	5.25	92.94	97.39
8	3b	350.37	5	4	1	2.56	75.71	1	-1.30	0.16	94.23	96.52
9	10b	402.88	6	3	1	5.65	55.12	1	0.66	2.10	100.00	97.57
10	3d	392.45	8	4	1	3.84	75.71	0	-1.09	0.04	87.27	96.41
11	4d	364.40	6	4	2	3.16	86.71	0	-0.79	0.026	86.19	96.86
12	11c	382.46	7	3	1	5.24	55.12	1	0.10	3.12	98.06	97.41
13	3c	364.40	6	4	1	2.83	75.71	0	-1.13	0.13	63.38	96.50
14	11e	410.52	9	3	1	6.25	55.12	1	0.14	0.13	100.00	97.49
15	9e	440.54	10	4	1	6.31	64.36	1	0.39	0.19	97.86	97.46
16	9c	412.49	8	4	1	5.30	64.36	1	0.32	1.13	94.88	97.46
17	9b	398.46	7	4	1	5.03	64.36	1	0.18	2.82	91.48	97.48
18	10d	430.94	8	3	1	6.43	55.12	1	0.83	0.36	100.00	97.68
19	9d	426.52	9	4	1	5.80	64.36	1	0.39	0.65	96.20	97.45
20	4e	384.39	3	4	2	3.67	86.71	0	-0.06	0.36	97.73	97.08
21	11d	396.49	8	3	1	5.75	55.12	1	0.14	0.53	99.52	97.45
22	9a	446.51	6	4	1	6.70	64.36	1	-0.97	0.23	100.00	97.64
23	3e	398.42	4	3	1	3.93	75.71	0	0.53	0.10	96.32	96.31
24	10a	450.93	5	3	1	7.32	55.12	1	-0.58	0.40	100.00	97.97
25	11a	416.48	5	3	1	6.64	55.12	1	-0.94	0.43	100.00	97.73

LogP: logarithm of compound partition coefficient between n-octanol and water.

M.Wt: molecular weight.

HBA: number of hydrogen bond acceptors.

HBD: number of hydrogen bond donors.

HBA: number of hydrogen bond acceptors.

TPSA: polar surface area.

BBB: Blood Brain Barrier.

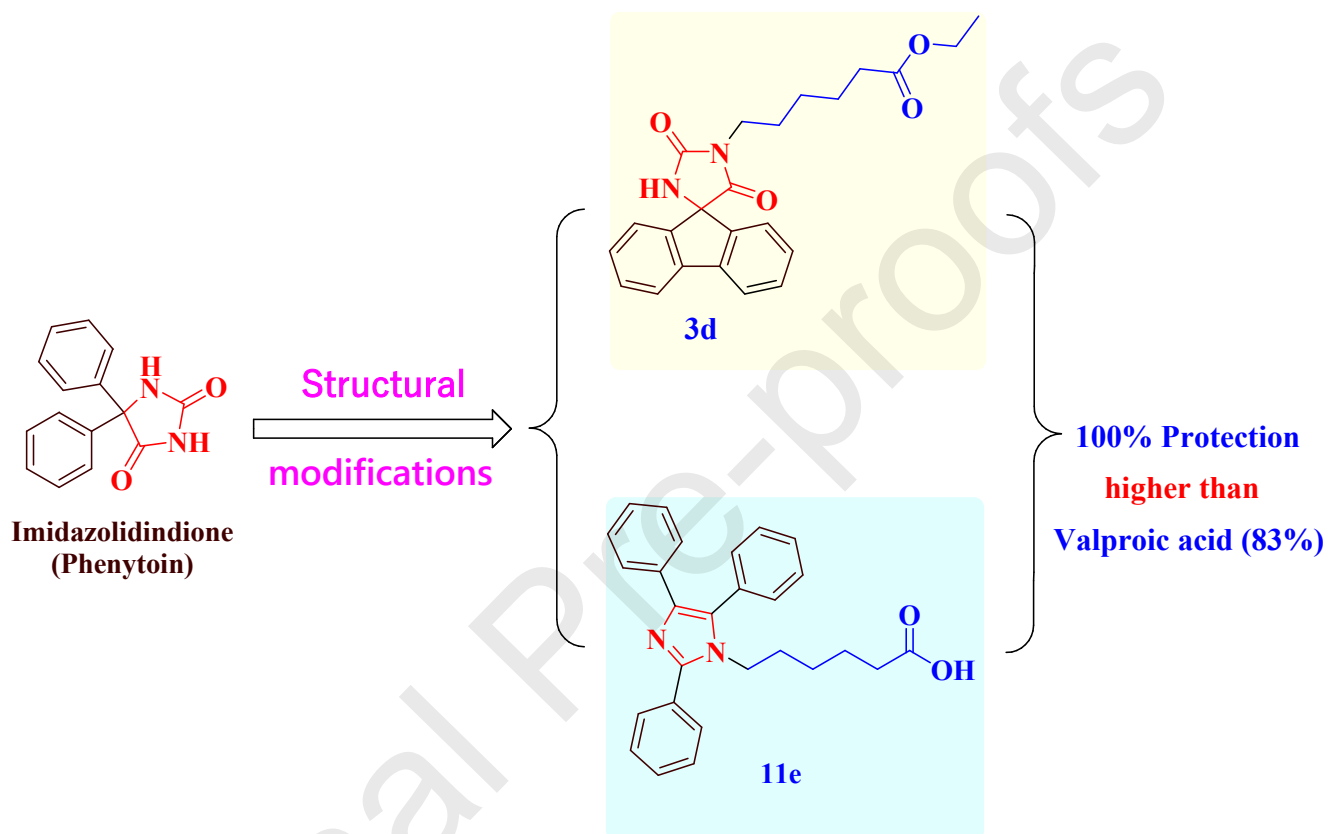
PPB: plasma protein binding

NRB: number of rotation bonds.

HIA: Percentages of human intestinal absorption

Graphical Abstract

Design, synthesis and anticonvulsant activity of new imidazolidindione and imidazole derivatives



Highlights

Title: Design, synthesis and anticonvulsant activity of new imidazolidindione and imidazole derivatives

Highlights

- New imidazolidindione and tetrasubstituted imidazole derivatives were synthesized and structurally approved.
- The anticonvulsant activity of the target compounds was evaluated in mice against electroshock and chemoshock.
- The neurotoxicity and protection against mortality from electroshock were also determined.
- The compounds showed excellent activities and specificity in chemoshock rather than electroshock.
- Some compounds showed more anticonvulsant activities than that of valproate with no neurotoxicity.
- Shape similarity using ROCS technique and physiochemical parameters were employed.
- Based on ROCS visualization and TC scores, these compounds have high similarity to hydantoin and valproic acid.